Chapter 10
Micromechanics of Composites

In this chapter we consider the results of incorporating a reinforcement (fibers, whiskers, particles, etc.) in a matrix to make a composite. It is of great importance to be able to predict the properties of a composite, given the properties of the components and the geometric arrangement of the components in the composite. We examine various micromechanical aspects of composites. A particularly simple case is the *rule-of-mixtures*, a rough tool that considers the composite properties as volume-weighted averages of the component properties. It is important to realize that the rule-of-mixtures works in only certain simple situations. Composite density is an example where the rule-of-mixtures is applied readily. In the case of mechanical properties, there are certain restrictions to its applicability. When more precise information is desired, it is better to use more sophisticated approaches based on the theory of elasticity.

10.1 Density

Consider a composite of mass m_c and volume v_c. The total mass of the composite is the sum total of the masses of fiber and matrix, that is,

$$m_c = m_f + m_m. \tag{10.1}$$

The subscripts c, f, and m indicate composite, fiber, and matrix, respectively. Note that Eq. (10.1) is valid even in the presence of any voids in the composite. The volume of the composite, however, must include the volume of voids, v_v. Thus,

$$v_c = v_f + v_m + v_v. \tag{10.2}$$

K.K. Chawla, *Composite Materials: Science and Engineering*,
DOI 10.1007/978-0-387-74365-3_10,

Dividing Eq. (10.1) by m_c and Eq. (10.2) by v_c and denoting the mass and volume fractions by M_f, M_m and V_f, V_m, V_v, respectively, we can write

$$M_f + M_m = 1 \tag{10.3}$$

and

$$V_f + V_m + V_v = 1. \tag{10.4}$$

The composite density ρ_c ($= m_c/v_c$) is given by

$$\rho_c = \frac{m_c}{v_c} = \frac{m_f + m_m}{v_c} = \frac{\rho_f v_f + \rho_m v_m}{v_c}$$

or

$$\rho_c = \rho_f V_f + \rho_m V_m. \tag{10.5}$$

We can also derive an expression for ρ_c in terms of mass fractions. Thus,

$$\begin{aligned}\rho_c &= \frac{m_c}{v_c} = \frac{m_c}{v_f + v_m + v_v} = \frac{m_c}{m_f/\rho_f + m_m/\rho_m + v_v} \\ &= \frac{1}{M_f/\rho_f + M_m/\rho_m + v_v/m_c} \\ &= \frac{1}{M_f/\rho_f + M_m/\rho_m + v_v/\rho_c v_c} \\ &= \frac{1}{M_f/\rho_f + M_m/\rho_m + V_v/\rho_c}.\end{aligned} \tag{10.6}$$

We can use Eq. (10.6) to indirectly measure the volume fraction of voids in a composite. Rewriting Eq. (10.6), we obtain

$$\rho_c = \frac{\rho_c}{\rho_c\left[M_f/\rho_f + M_m/\rho_m\right] + V_v}$$

or

$$V_v = 1 - \rho_c\left(\frac{M_f}{\rho_f} + \frac{M_m}{\rho_m}\right). \tag{10.7}$$

Example 10.1 A thermoplastic matrix contains 40 wt.% glass fiber. If the density of the matrix, ρ_m, is 1.1 g/cm^3 while that of glass fiber, ρ_f, is 2.5 g/cm^3, what is the density of the composite? Assume that no voids are present.

Solution Consider 100 g of the composite:

$$\text{Amount of glass fiber, } m_f = 40\,\text{g}$$
$$\text{Amount of matrix, } m_m = 60\,\text{g}.$$

Volume of the composite, v_c is the sum of the volumes of fiber, v_f and matrix, v_m

$$\begin{aligned} v_c &= v_m + v_f \\ &= (m_m/\rho_m) + \left(m_f/\rho_f\right) = (60/1.1 + 40/2.5)\text{cm}^3 \\ &= 54.5 + 16 = 70.5\,\text{cm}^3. \end{aligned}$$

The density of the composite, is

$$\rho_c = 100\,\text{g}/70.5\,\text{cm}^3 = 1.42\,\text{g/cm}^3.$$

10.2 Mechanical Properties

In this section, we first describe some of the methods for predicting elastic constants, thermal properties, and transverse stresses in fibrous composites and then we treat the mechanics of load transfer.

10.2.1 Prediction of Elastic Constants

Consider a unidirectional composite such as the one shown in Fig. 10.1. Assume that plane sections of this composite remain plane after deformation. Let us apply a force P_c in the fiber direction. Now, if the two components adhere perfectly and if they have the same Poisson's ratio, then each component will undergo the same longitudinal elongation, Δl. Thus, we can write for the strain in each component

$$\varepsilon_f = \varepsilon_m = \varepsilon_{cl} = \frac{\Delta l}{l}, \tag{10.8}$$

where ε_{cl} is the strain in the composite in the longitudinal direction. This is called the *isostrain* or *action-in-parallel* situation. It was first treated by Voigt (1910). If both fiber and matrix are elastic, we can relate the longitudinal stress σ in the two components to the longitudinal strain ε_l by Young's modulus E. Thus,

$$\sigma_f = E_f \varepsilon_{cl} \quad \text{and} \quad \sigma_m = E_m \varepsilon_{cl}.$$

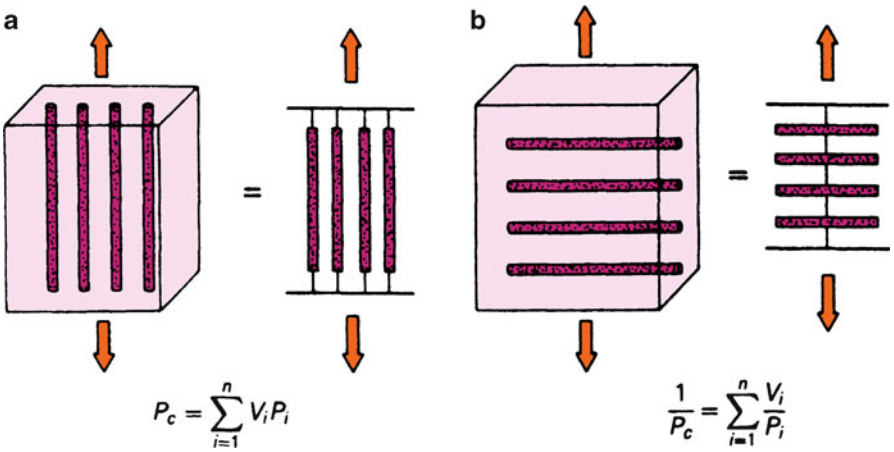

Fig. 10.1 Unidirectional composite: (**a**) isostrain or action in parallel and (**b**) isostress or action in series

Let A_c be the cross-sectional area of the composite, A_m, that of the matrix, and A_f, that of all the fibers. The applied load on the composite, P_c is shared between the fiber and the matrix. We can write

$$P_c = P_f + P_m,$$

where P_f and P_m are the loads on the fiber and the matrix, respectively. Converting into stress components, we can write

$$\sigma_{cl} A_c = \sigma_f A_f + \sigma_m A_m. \tag{10.9}$$

From Eqs. (10.8) and (10.9), we get

$$\sigma_{cl} A_c = \left(E_f A_f + E_m A_m\right) \varepsilon_{cl}$$

or

$$E_{cl} = \frac{\sigma_{cl}}{\varepsilon_{cl}} = E_f \frac{A_f}{A_c} + E_m \frac{A_m}{A_c},$$

where E_{cl} is the longitudinal Young's modulus of the composite. The longitudinal modulus is also denoted by E_{11}.

Now, for a given length of a composite, $A_f/A_c = V_f$ and $A_m/A_c = V_m$. Then the preceding expression can be simplified to

$$E_{cl} = E_f V_f + E_m V_m = E_{11}. \tag{10.10}$$

Equation (10.10) is called the rule-of-mixtures for Young's modulus in the fiber direction.

A similar expression can be obtained for the composite longitudinal strength from (10.9), namely,

$$\sigma_{cl} = \sigma_f V_f + \sigma_m V_m. \tag{10.11}$$

For properties in the transverse direction, we can represent the simple unidirectional composite by what is called the *action-in-series* or *isostress* situation; see Fig. 10.1b. In this case, we group the fibers together as a continuous phase normal to the stress. Thus, we have equal stresses in the two components and the model is equivalent to that treated by Reuss (1929). For loading transverse to the fiber direction, we have for isostress

$$\sigma_{ct} = \sigma_f = \sigma_m$$

while the total displacement of the composite in the thickness direction, Δt_c, is the sum of displacements of the matrix and fiber, that is,

$$\Delta t_c = \Delta t_m + \Delta t_f.$$

Dividing throughout by t_c, the gage length of the composite, we obtain

$$\frac{\Delta t_c}{t_c} = \frac{\Delta t_m}{t_c} + \frac{\Delta t_f}{t_c}.$$

Now $\Delta t_c/t_c = \varepsilon_{ct}$, strain in the composite in the transverse direction, while Δt_m and Δt_f equal the strains in the matrix and fiber times their respective gage lengths; that is, $\Delta t_m = \varepsilon_m t_m$ and $\Delta t_f = \varepsilon_f t_f$. Then

$$\varepsilon_{ct} = \frac{\Delta t_c}{t_c} = \frac{\Delta t_m}{t_m}\frac{t_m}{t_c} + \frac{\Delta t_f}{t_f}\frac{t_f}{t_c}$$

or

$$\varepsilon_{ct} = \varepsilon_m \frac{t_m}{t_c} + \varepsilon_f \frac{t_f}{t_c}. \tag{10.12}$$

For a given cross-sectional area of the composite under the applied load, the volume fractions of fiber and matrix can be written as

$$V_m = \frac{t_m}{t_c} \quad \text{and} \quad V_f = \frac{t_f}{t_c}.$$

This simplifies Eq. (10.12) to

$$\varepsilon_{ct} = \varepsilon_m V_m + \varepsilon_f V_f. \tag{10.13}$$

Considering both components to be elastic and remembering that $\sigma_{ct} = \sigma_f = \sigma_m$ in this case, we can write (10.13) as

$$\frac{\sigma_{ct}}{E_{ct}} = \frac{\sigma_{ct}}{E_m} V_m + \frac{\sigma_{ct}}{E_f} V_f$$

or

$$\frac{1}{E_{ct}} = \frac{V_m}{E_m} + \frac{V_f}{E_f} = \frac{1}{E_{22}}. \tag{10.14}$$

The relationships given by Eqs. (10.5), (10.10), (10.11), (10.13), and (10.14) are commonly referred to as rules-of-mixtures (volume weighted averages). Figure 10.2 shows the plots of Eqs. (10.10) and (10.14). The reader should appreciate that these relationships and their variants are but rules-of-thumb obtained from a simple, strength of materials approach. More comprehensive micromechanical models, based on the theory of elasticity, can and should be used to obtain the elastic constants of fibrous composites. We describe below, albeit very briefly, some of these.

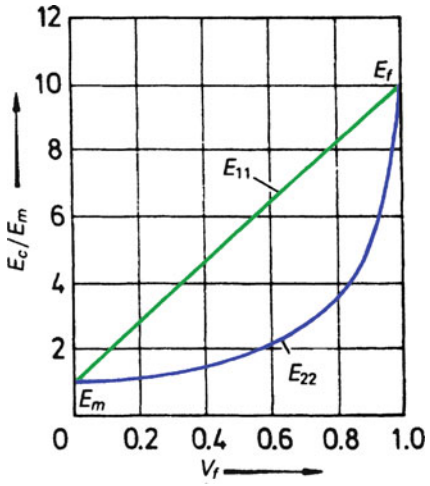

Fig. 10.2 Variation of longitudinal modulus (E_{11}) and transverse modulus (E_{22}) with fiber volume fraction (V_f)

10.2.2 Micromechanical Approaches

The states of stress and strain can each be described by six components. An anisotropic body with no symmetry elements present requires 21 independent elastic constants to relate stress and strain (Nye 1985). This is the most general case of elastic anisotropy. An elastically isotropic body, on the other hand, is the simplest case; it needs only two independent elastic constants. In such a body, when a tensile

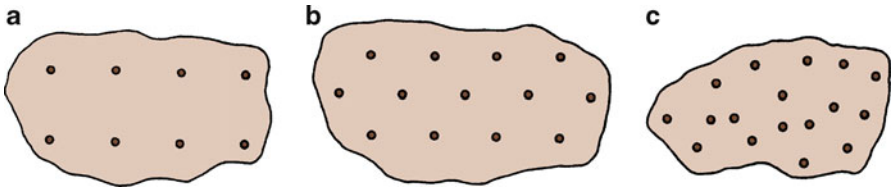

Fig. 10.3 Various fiber arrays in a matrix: (**a**) square, (**b**) hexagonal, and (**c**) random

stress σ_z is applied in the z direction, a tensile strain ε_z results in that direction. In addition to this tensile strain, there are two equal compressive strains ($\varepsilon_x = \varepsilon_y$) in the x and y directions. In a generally anisotropic body, the two transverse strain components are not equal. In fact, as we shall see in Chap. 11, in such a body, tensile loading can result in tensile and shear strains. The large number of independent elastic constants (21 in the most general case, i.e., no symmetry elements) represents the degree of elastic complexity in a given system. Any symmetry elements present will reduce the number of independent elastic constants (Nye 1985).

A composite containing uniaxially aligned fibers will have a plane of symmetry perpendicular to the fiber direction (i.e., material on one side of the plane will be the mirror image of the material on the other side). Figure 10.3 shows square, hexagonal, and random fiber arrays in a matrix. A square array of fibers, for example, will have symmetry planes parallel to the fibers as well as perpendicular to them. Such a material is an orthotropic material (three mutually perpendicular planes of symmetry) and possesses nine independent elastic constants (Nye 1985). Hexagonal and random arrays of aligned fibers are transversely isotropic and have five independent elastic constants. These five constants as well as the stress–strain relationships, as derived by Hashin and Rosen (1964) and Rosen (1973), are given in Table 10.1. There are two Poisson's ratios: one gives the transverse strain caused by an axially applied stress, and the other gives the axial strain caused by a transversely applied stress. The two are not independent but are related (see Sect. 11.3). Thus, the number of independent elastic constants for a transversely isotropic composite is five. Note that the total number of independent elastic constants in Table 10.1 is five (count the number of *C*s).

More accurate results can be obtained if we take into account the inevitable scatter in the distribution of fibers, i.e., in reality, they never have an idealized distribution in the matrix. A summary of the elastic constants for a transversely isotropic composite (see Fig. 10.4) in terms of the elastic constants of the two components is given in Table 10.2 (Chamis 1983). Note the use of $\sqrt{V_f}$ in these expressions. Because the plane 2–3 is isotropic in Fig. 10.4, the properties in directions 2 and 3 are identical. The matrix is treated as an isotropic material while the fiber is treated as an anisotropic material. Thus, E_m and ν_m are the two constants required for the matrix while five constants (E_{f1}, E_{f2}, G_{f12}, G_{f23}, and ν_{f12}) are required for the fiber. The expressions for the five independent constants (E_{11}, E_{22}, G_{12}, G_{23}, and ν_{12}) are given in Table 10.2. The two Poisson's ratios are not independent (see Chap. 11).

Frequently, composite structures are fabricated by stacking thin sheets of unidirectional composites called *plies* in an appropriate orientation sequence

Table 10.1 Elastic moduli of a transversely isotropic fibrous composite

$E = C_{11} - \dfrac{2C_{12}^2}{C_{22} + C_{23}}$	$K_{23} = \dfrac{1}{2}(C_{22} + C_{23})$
$G = G_{12} = G_{13} = G_{44}$	$G_{23} = \dfrac{1}{2}(C_{22} - C_{23})$
$v = v_{13} = v_{31} = \dfrac{1}{2}\left(\dfrac{C_{11} - E}{K_{23}}\right)^{1/2}$	$v_{23} = \dfrac{K_{23} - \phi G_{23}}{K_{23} + \phi G_{23}}$
$E_2 = E_3 = \dfrac{4G_{23}K_{23}}{K_{23} + \phi G_{23}}$	$\phi = 1 + \dfrac{4K_{23}v^2}{E}$
Stress–strain relationships	
$\varepsilon_{11} = \dfrac{1}{E_1}[\sigma_{11} - v(\sigma_{22} + \sigma_{33})]$	$\varepsilon_{22} = \varepsilon_{33} = \dfrac{1}{E_2}(\sigma_{22} - v\sigma_{33}) - \dfrac{v}{E}\sigma_{11}$
$\gamma_{12} = \gamma_{13} = \dfrac{1}{G}\sigma_{12}$	$\gamma_{23} = \dfrac{2(1 + v_{23})}{E_2}\sigma_{23}$

Source: Adapted with permission from Hashin and Rosen (1964)

Table 10.2 Elastic constants of a transversely isotropic composite in terms of component constants (matrix isotropic, fiber anisotropic)

Longitudinal modulus	$E_{11} = E_{f1}V_f + E_mV_m$
Transverse modulus	$E_{22} = E_{33} = \dfrac{E_m}{1 - \sqrt{V_f}(1 - E_m/E_{f2})}$
Shear modulus	$G_{12} = G_{13} = \dfrac{G_m}{1 - \sqrt{V_f}(1 - G_m/G_{f12})}$
Shear modulus	$G_{23} = \dfrac{G_m}{1 - \sqrt{V_f}(1 - G_m/G_{f23})}$
Poisson's ratio	$v_{12} = v_{13} = v_{f12}V_f + v_mV_m$
Poisson's ratio	$v_{23} = \dfrac{E_{22}}{2G_{23}} - 1$

Source: Adapted with permission from Chamis (1983)

dictated by elasticity theory (see Chap. 11). It is of interest to know properties, such as the elastic constants and the strength characteristics of a ply. In particular, it is very valuable if we are able to predict the lamina characteristics starting from the characteristics of the individual components. Later in the macro-mechanical analysis (Chap. 11), we treat a ply as a homogeneous but thin orthotropic material. Elastic constants in the thickness direction can be ignored in such a ply, leaving four independent elastic constants, namely, E_{11}, E_{22}, v_{12}, and G_{12}, i.e., one less than the number of constants required for a thick but transversely isotropic material. The missing constant is G_{23}, the transverse shear modulus in the 2–3 plane, normal to the fiber axis. A brief description of the various micromechanical techniques used to predict the elastic constants follows and then we give an account of a set of empirical equations, called *Halpin-Tsai equations*, that can be used under certain conditions to predict the elastic constants of a fiber composite.

In the so-called *self-consistent field methods* (Chamis and Sendecky 1968), approximations of phase geometries are made and a simple representation of the

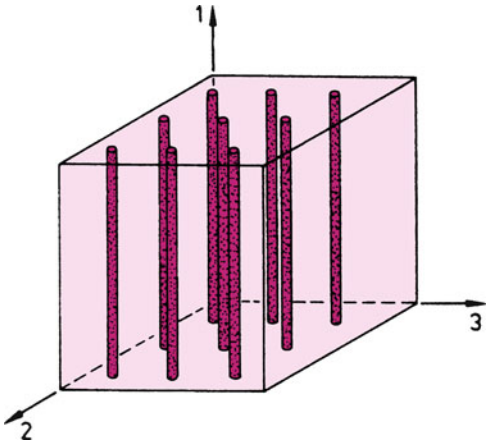

Fig. 10.4 A transversely isotropic fiber composite: plane transverse to fibers (2–3 plane) is isotropic

response field is obtained. The phase geometry is represented by one single fiber embedded in a matrix cylinder. This outer cylinder is embedded in an unbounded homogeneous material whose properties are taken to be equivalent to those of average composite properties. The matrix under a uniform load at infinity introduces a uniform strain field in the fiber. Elastic constants are obtained from this strain field. The results obtained are independent of fiber arrangements in the matrix and are reliable at low-fiber-volume fractions (V_f), reasonable at intermediate V_f, and unreliable at high V_f (Hill 1964). *Exact methods* deal with specific geometries, for example, fibers arranged in a hexagonal, square, or rectangular array in a matrix. The elasticity problem is then solved by a series development, a complex variable technique, or a numerical solution. The approach of Eshelby (1957, 1959) considers an infinite matrix containing an ellipsoidal inclusion. Modifications of the Eshelby method have been made by Mori and Tanaka (1973).

The *variational or bounding methods* focus on the upper and lower bounds on elastic constants. When the upper and lower bounds coincide, the property is determined exactly. Frequently, the upper and lower bounds are well separated. When these bounds are close enough, we can safely use them as indicators of the material behavior. It turns out that this is the case for longitudinal properties of a unidirectional lamina. Hill (1965) derived bounds for the ply elastic constants that are analogous to those derived by Hashin and Rosen (1964) and Rosen (1973). In particular, Hill put rigorous bounds on the longitudinal Young's modulus, E_{11}, in terms of the bulk modulus in plane strain (k_p), Poisson's ratio (v), and the shear modulus (G) of the two phases. No restrictions were made on the fiber form or packing geometry. The term k_p is the modulus for lateral dilation with zero longitudinal strain and is given by

$$k_p = \frac{E}{2(1-2v)(1+v)}.$$

The bounds on the longitudinal modulus, E_{11}, are

$$\frac{4V_fV_m\left(v_f - v_m\right)^2}{\left(V_f/k_{\text{pm}}\right) + \left(V_m/k_{\text{pf}}\right) + 1/G_m} \leq E_{11} - E_fV_f - E_mV_m \leq \frac{4V_fV_m\left(v_f - v_m\right)^2}{\left(V_f/k_{\text{pm}}\right) + \left(V_m/k_{\text{pf}}\right) + 1/G_f} \tag{10.15}$$

Equation (10.15) shows that the deviations from the rule-of-mixtures (10.10) are quite small (<2 %). We may verify this by substituting some values of practical composites such as carbon or boron fibers in an epoxy matrix or a metal matrix composite such as tungsten in a copper matrix. Note that the deviation from the rule-of-mixtures value comes from the $(v_{\text{m}} - v_{\text{f}})^2$ factor. For $v_{\text{f}} = v_{\text{m}}$, we have E_{11} given exactly by the rule-of-mixtures.

Hill (1965) also showed that for a unidirectionally aligned fiber composite

$$v_{12} \gtrless v_fV_f + v_mV_m \quad \text{accordingly as} \quad (v_f - v_m)(k_{\text{pf}} - k_{\text{pm}}) \gtrless 0 \tag{10.16}$$

Generally, $v_{\text{f}} < v_{\text{m}}$ and $E_{\text{f}} >> E_{\text{m}}$. Then, v_{12} will be less than that predicted by the rule-of-mixtures ($= v_{\text{f}}V_{\text{f}} + v_{\text{m}}V_{\text{m}}$). It is easy to see that the bounds on v_{12} are not as close as the ones on E_{11}. This is because $v_{\text{f}} - v_{\text{m}}$ appears in the case of v_{12} (10.16) while $(v_{\text{f}} - v_{\text{m}})^2$ appears in the case of E_{11} (10.15). In the case where $v_{\text{f}} - v_{\text{m}}$ is very small, the bounds are close enough to allow us to write

$$v_{12} \approx v_fV_f + v_mV_m. \tag{10.17}$$

10.2.3 Halpin-Tsai Equations

Halpin, Tsai, and Kardos (Halpin and Tsai 1967; Halpin and Kardos 1976; Kardos 1971) empirically developed some generalized equations that readily give satisfactory results compared to the complicated expressions. They are also useful in determining the properties of composites that contain discontinuous or short fibers oriented in the loading direction. One writes a single equation of the form

$$\frac{p}{p_m} = \frac{1 + \xi\eta V_f}{1 - \eta V_f}, \tag{10.18}$$

$$\eta = \frac{p_f/p_m - 1}{p_f/p_m + \xi}, \tag{10.19}$$

Table 10.3 Values of ξ for some uniaxial composites

Modulus	ξ
E_{11}	$2(l/d)$
E_{22}	0.5
G_{12}	1.0
G_{21}	0.5
K	0

Source: Adapted from Nielsen (1974), courtesy of Marcel Dekker, Inc.

where p represents one of the moduli of composite, for example, E_{11}, E_{22}, G_{12}, or G_{23}; p_{m} and p_{f} are the corresponding modulus of the matrix and fiber, respectively; V_{f} is the fiber volume fraction; and ξ is a measure of the reinforcement that depends on boundary conditions (fiber geometry, fiber distribution, and loading conditions). The term ξ is an empirical factor that is used to make Eq. (10.18) conform to the experimental data.

The function η in Eq. (10.19) is constructed in such a way that when $V_{\mathrm{f}} = 0$, $p = p_{\mathrm{m}}$ and when $V_{\mathrm{f}} = 1$, $p = p_{\mathrm{f}}$. Furthermore, the form of η is such that

$$\frac{1}{p} = \frac{V_m}{p_m} + \frac{V_f}{p_f} \quad \text{for} \quad \xi \to 0$$

and

$$p = p_f V_f + p_m V_m \quad \text{for} \quad \xi \to \infty.$$

These two extremes (not necessarily tight) bound the composite properties. Thus, values of ξ between 0 and ∞ will give an expression for p between these extremes. Some typical values of ξ are given in Table 10.3. Thus, we can cast the Halpin-Tsai equations for the transverse modulus as

$$\frac{E_{22}}{E_m} = \frac{1 + \xi\eta V_f}{1 - \eta V_f} \quad \text{and} \quad \eta = \frac{E_f/E_m - 1}{E_f/E_m + \xi}. \tag{10.20}$$

Comparing these expressions with exact elasticity solutions, one can obtain the value of ξ. Whitney (1973) suggests $\xi = 1$ or 2 for E_{22}, depending on whether a hexagonal or square array of fibers is used.

Nielsen (1974) modified the Halpin-Tsai equations to include the maximum packing fraction $\phi_{\max}$ of the reinforcement. His equations are

$$\begin{aligned} \frac{p}{p_m} &= \frac{1 + \xi\eta V_f}{1 - \eta\Psi V_f}, \\ \eta &= \frac{p_f/p_m - 1}{p_f/p_m + \xi}, \\ \Psi &\simeq 1 + \left(\frac{1 - \phi_{\max}}{\phi_{\max}^2}\right) V_f, \end{aligned} \tag{10.21}$$

where $\phi_{\max}$ is the maximum packing factor. It allows one to take into account the maximum packing fraction. For a square array of fibers, $\phi_{\max} = 0.785$, while for a hexagonal arrangement of fibers, $\phi_{\max} = 0.907$. In general, $\phi_{\max}$ is between these two extremes and near the random packing, $\phi_{\max} = 0.82$.

Example 10.2 Consider a unidirectionally reinforced glass fiber/epoxy composite. The fibers are continuous and 60 % by volume. The tensile strength of glass fibers is 1 GPa and the Young's modulus is 70 GPa. The tensile strength of the epoxy matrix is 60 MPa and its Young's modulus is 3 GPa. Compute the Young's modulus and the tensile strength of the composite in the longitudinal direction.

Solution Young's modulus of the composite in the longitudinal direction is given by

$$E_{cl} = 70 \times 0.6 + 3 \times 0.4 = 42 + 1.2 = 43.2 \text{ GPa}.$$

To calculate the tensile strength of the composite in the longitudinal direction, we need to determine which component, fiber or matrix, has the lower failure strain. The failure strain of the fiber is

$$\varepsilon_f = \sigma_f / E_f = 1/70 = 0.014$$

while that of the matrix is

$$\varepsilon_m = \left(60 \times 10^{-3}\right)/3 = 0.020.$$

Thus, $\varepsilon_{\mathrm{f}} < \varepsilon_{\mathrm{m}}$, i.e., fibers fail first. At that strain, assuming a linear stress–strain curve for the epoxy matrix, the matrix strength is $\sigma'_m = E_m \varepsilon_f = 3 \times 0.014 = 0.042$ GPa. Then, we get the composite tensile strength as

$$\begin{aligned} \sigma_c &= 0.6 \times 1 + 0.4 \times 0.042 \\ &= 0.6 + 0.0168 = 617 \text{ MPa}. \end{aligned}$$

10.2.4 Transverse Stresses

When a fibrous composite consisting of components with different elastic moduli is uniaxially loaded, stresses in transverse directions arise because of the difference in Poisson's ratio of the matrix and the fiber, that is, because the two components have different contractile tendencies. Here we follow Kelly's (1970) treatment of this important but, unfortunately, not well-appreciated subject. This problem in

elasticity is also useful in computing thermal stresses in composites; in which case the two components have different thermal expansion coefficients.

Consider a unit fiber reinforced composite consisting of a single fiber (radius a) surrounded by its shell of matrix (outer radius b) as shown in Fig. 10.5. The composite as a whole is thought to be built of an assembly of such unit composites, a reasonably valid assumption at moderate fiber volume fractions. We axially load the composite in direction z. Owing to the obvious cylindrical symmetry, we treat the problem in polar coordinates, r, θ, and z. It follows from the axial symmetry that the stress and strain are independent of angle θ and are functions only of r, which simplifies the problem. We can write Hooke's law for this situation as

$$\begin{bmatrix} e_r & 0 & 0 \\ 0 & e_\theta & 0 \\ 0 & 0 & e_z \end{bmatrix} = \frac{1+v}{E} \begin{bmatrix} \sigma_r & 0 & 0 \\ 0 & \sigma_\theta & 0 \\ 0 & 0 & \sigma_z \end{bmatrix} - \frac{v}{E}(\sigma_r + \sigma_\theta + \sigma_z) \begin{bmatrix} 1 & 0 & 0 \\ 0 & 1 & 0 \\ 0 & 0 & 1 \end{bmatrix} \quad (10.22)$$

where e is the strain, σ is the stress, v is the Poisson's ratio, E is Young's modulus in the longitudinal direction, and the subscripts r, θ, and z refer to the radial, circumferential, and axial directions, respectively. The only equilibrium equation for this problem is

$$\frac{\mathrm{d}\sigma_r}{\mathrm{d}r} + \frac{\sigma_r - \sigma_\theta}{r} = 0. \quad (10.23)$$

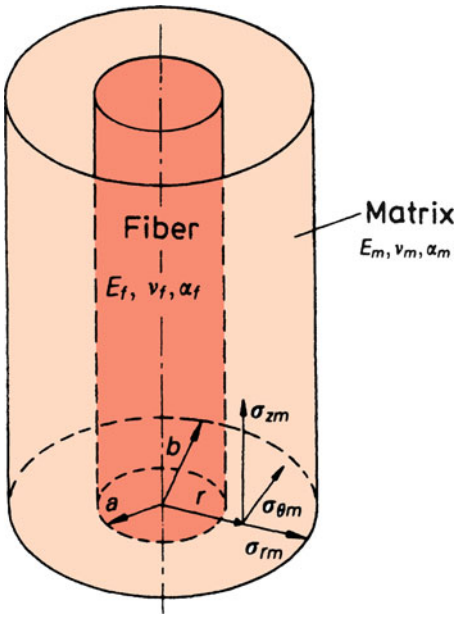

Fig. 10.5 A single fiber surrounded by its matrix shell

Also, for the plane strain condition, we can write for the strain components, in terms of displacements,

$$e_r = \frac{\mathrm{d}u_r}{\mathrm{d}r}, \qquad e_\theta = \frac{u_r}{r}, \qquad e_z = \text{const} \tag{10.24}$$

where u_r is the radial displacement.

From Eq. (10.22) we have, after some algebraic manipulation,

$$\begin{aligned} \frac{\sigma_\theta}{K} &= (1-v)e_\theta + v(e_r + e_z), \\ \frac{\sigma_r}{K} &= (1-v)e_r + v(e_\theta + e_z), \end{aligned} \tag{10.25}$$

where

$$K = \frac{E}{(1+v)(1-2v)}.$$

From Eqs. (10.24) and (10.25), we get

$$\begin{aligned} \frac{\sigma_\theta}{K} &= v\frac{\mathrm{d}u_r}{\mathrm{d}r} + (1-v)\frac{u_r}{r} + ve_z, \\ \frac{\sigma_r}{K} &= (1-v)\frac{\mathrm{d}u_r}{\mathrm{d}r} + v\frac{u_r}{r} + ve_z. \end{aligned} \tag{10.26}$$

Substituting Eq. (10.26) in Eq. (10.23), we obtain the following differential equation in terms of the radial displacement u_r:

$$\frac{\mathrm{d}^2u_r}{\mathrm{d}r^2} + \frac{1}{r}\frac{\mathrm{d}u_r}{\mathrm{d}r} - \frac{u_r}{r^2} = 0. \tag{10.27}$$

Equation (10.27) is a common differential equation in elasticity problems with rotational symmetry (Love 1952), and its solution is

$$u_r = Cr + \frac{C'}{r} \tag{10.28}$$

where C and C' are constants of integration to be determined by using boundary conditions. Now, Eq. (10.28) is valid for displacements in both components, that is, fiber and matrix. Let us designate the central component by subscript 1 and the sleeve by subscript 2. Thus, we can write the displacements in the two components as

$$\begin{aligned} u_{r1} &= C_1 r + \frac{C_2}{r}, \\ u_{r2} &= C_3 r + \frac{C_4}{r}. \end{aligned} \tag{10.29}$$

The boundary conditions for our problem can be expressed as follows:

1. At the free surface, the stress is zero, that is, $\sigma_{r2} = 0$ at $r = b$.
2. At the interface, the continuity condition requires that at $r = a$, $u_{r1} = u_{r2}$ and $\sigma_{r1} = \sigma_{r2}$.
3. The radial displacement must vanish along the symmetry axis, that is, at $r = 0$, $u_{r1} = 0$.

The last boundary condition immediately gives $C_2 = 0$, because otherwise u_{r1} will become infinite at $r = 0$. By applying the other boundary conditions to Eqs. (10.26) and (10.29), we obtain three equations with three unknowns. Knowing these integration constants, we obtain u_r and thus the stresses in the two components. It is convenient to develop an expression for radial pressure p at the interface. At the interface $r = a$, if we equate σ_{r2} to $-p$, then after some tedious manipulations it can be shown that

$$p = \frac{2e_z(v_2 - v_1)V_2}{V_1/k_{p2} + V_2/k_{p1} + 1/G_2}, \tag{10.30}$$

where k_p is the plane strain bulk modulus equal to $E/2(1 + v)(1 - 2v)$ while the subscripts 1 and 2 refer to the two components. The expressions for the stresses in the components involving radial pressure, p are

Component 1:

$$\begin{aligned} \sigma_{r1} &= \sigma_{\theta 1} = -p, \\ \sigma_{z1} &= E_1 e_z - 2v_1 p. \end{aligned} \tag{10.31}$$

Component 2:

$$\begin{aligned} \sigma_{r2} &= p\left(\frac{a^2}{b^2 - a^2}\right)\left(1 - \frac{b^2}{r^2}\right), \\ \sigma_{\theta 2} &= p\left(\frac{a^2}{b^2 - a^2}\right)\left(1 + \frac{b^2}{r^2}\right), \\ \sigma_{z2} &= E_2 e_z + 2v_2 p\left(\frac{a^2}{b^2 - a^2}\right). \end{aligned} \tag{10.32}$$

Note that p is positive when the central component 1 is under compression, that is, when $v_1 < v_2$.

Figure 10.6 shows the stress distribution schematically in a fiber composite (1 = fiber, 2 = matrix). We can draw some inferences from Eqs. (10.31) and (10.32) and Fig. 10.6.

1. Axial stress is uniform in components 1 and 2, although its magnitude is different in the two and depends on the respective elastic constants.

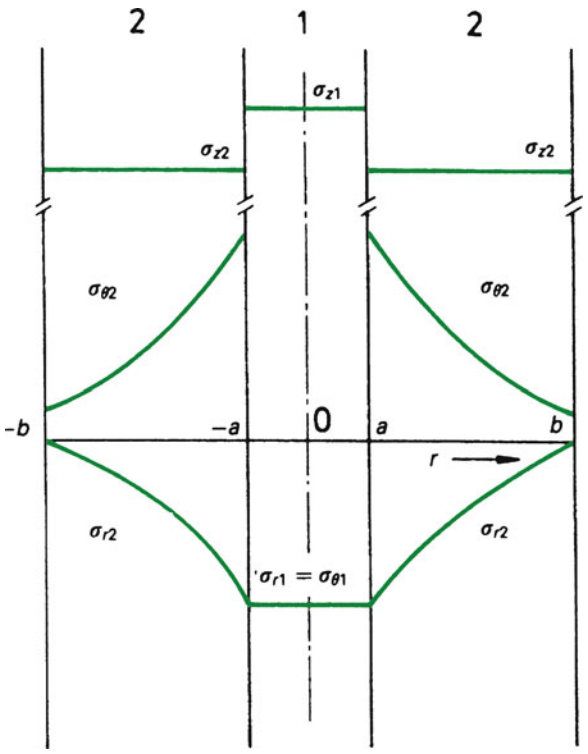

Fig. 10.6 Three-dimensional stress distribution (schematic) in the unit composite shown in Fig. 10.5. In this case, the transverse stresses (σ_r and σ_θ) result from the differences in the Poisson's ratios of the fiber and matrix

2. In the central component 1, σ_{r1} and $\sigma_{\theta 1}$ are equal in magnitude and sense. In the sleeve 2, σ_{r2} and $\sigma_{\theta 2}$ vary as $1 - b^2/r^2$ and $1 + b^2/r^2$, respectively.
3. When the Poisson's ratio difference ($\nu_2 - \nu_1$) goes to zero, σ_r and σ_θ go to zero; that is, the rheological interaction will vanish.
4. Because of the relatively small difference in the Poisson's ratio of the components of a composite, the transverse stresses that develop in the elastic regime will be relatively small. If one of the components deforms plastically ($\nu \rightarrow 0.5$), then $\Delta\nu$ can become significant and so will the transverse stresses.

10.3 Thermal Properties

Thermal energy is responsible for the atomic or molecular vibration about a mean position in any material. As the temperature of the materials is increased, the amplitude of thermal energy-induced vibrations is increased and the interatomic or intermolecular spacing increases, i.e., an expansion of the body occurs. Most materials show such an expansion with increasing temperature. In general, the thermal expansion of a material is greater in the liquid state than in the crystalline state, with the transition occurring at the melting point. In the case of

a glassy material, such a transition occurs at the glass transition temperature, although it is not as well defined as the one at the melting point. Over a certain range of temperature, one can relate the temperature interval and thermal strain by a coefficient, called the *coefficient of thermal expansion*. In the case of a linear strain, the linear thermal expansion coefficient, α, is a second-rank symmetric tensor, and is related to the strain tensor, ε, by the following relationship:

$$\varepsilon_{ij} = \alpha_{ij}\Delta T, \tag{10.33}$$

where ΔT is the temperature change. The two indexes indicate the second-rank tensor. The thermal expansion coefficient, α, generally does not have a constant value over a very large range of temperature. Thus, we can define α_{ij} in a more general way by taking into account this variation with temperature as follows:

$$\alpha_{ij} = \delta\varepsilon_{ij}/\delta T.$$

If we consider a volumetric strain, the volumetric coefficient of thermal expansion, β, is given by

$$\beta_{ij} = \frac{1}{V}\left(\frac{\delta V}{\delta T}\right),$$

where V is the volume and T is the temperature. For small strains, it can be easily shown that

$$\beta_{ij} = 3\alpha_{ij}.$$

Recall that the sum of the diagonal terms of the strain tensor is equal to volume change. Hence, the volumetric expansion coefficient, β, is equal to the sum of the diagonal terms of the strain tensor, i.e.,

$$\beta = \varepsilon_{11} + \varepsilon_{22} + \varepsilon_{33} = 3\alpha \tag{10.34a}$$

or

$$\alpha = \frac{1}{3}[\varepsilon_{11} + \varepsilon_{22} + \varepsilon_{33}]. \tag{10.34b}$$

As we said earlier, only over some specified range of temperature can the coefficient of thermal expansion (CTE) be treated as a constant. Consider a temperature range ΔT over which α is a constant. We can write Eq. (10.33) in an extended form as

$$\begin{vmatrix} \varepsilon_{11} & \varepsilon_{12} & \varepsilon_{13} \\ & \varepsilon_{22} & \varepsilon_{23} \\ & & \varepsilon_{33} \end{vmatrix} = \begin{vmatrix} \alpha_{11} & \alpha_{12} & \alpha_{13} \\ & \alpha_{22} & \alpha_{23} \\ & & \alpha_{23} \end{vmatrix} \Delta T. \tag{10.35a}$$

Or, using the contracted notation (see Sect. 11.1), we can write

$$\begin{vmatrix} \varepsilon_1 \\ \varepsilon_2 \\ \varepsilon_3 \\ \varepsilon_4 \\ \varepsilon_5 \\ \varepsilon_6 \end{vmatrix} = \begin{vmatrix} \alpha_1 \\ \alpha_2 \\ \alpha_3 \\ \alpha_4 \\ \alpha_5 \\ \alpha_6 \end{vmatrix} \Delta T \tag{10.35b}$$

If an arbitrary direction [*hkl*] has direction cosines n_1, n_2, and n_3, then we can write for the linear thermal expansion coefficient, α_{hkl}, in that direction

$$\alpha_{hkl} = n_1^2\alpha_1 + n_2^2\alpha_2 + n_3^2\alpha_3. \tag{10.36}$$

In a transversely isotropic fibrous composite (i.e., hexagonal symmetry), we have $\alpha_1 = \alpha_2 = \alpha_\perp$, perpendicular to the fiber axis and $\alpha_3 = \alpha_{||}$, parallel to the fiber axis. Then, remembering that $n_1^2 + n_2^2 + n_3^2 = 1$, Eq. (10.36) becomes

$$\alpha_{hkl} = \left(n_1^2 + n_2^2\right)\alpha_1 + n_3^2\alpha_3,$$

$$\alpha_{hkl} = \alpha_\perp \sin^2\theta + \alpha_{||}\cos^2\theta, \tag{10.37a}$$

$$\alpha_{hkl} = \alpha_\perp + \left(\alpha_{||} - \alpha_\perp\right)\cos^2\theta, \tag{10.37b}$$

where θ is the angle between direction [*hkl*] and the fiber axis.

10.3.1 Expressions for Coefficients of Thermal Expansion of Composites

Various expressions have been proposed that give the thermal expansion coefficients of a composite, knowing the material constants of the components and their geometric arrangements. Different expressions predict very different values of expansion coefficients for a given composite. Almost all expressions, however, predict expansion coefficient values that are different from those given by a simple rule-of-mixtures ($= \alpha_f V_f + \alpha_m V_m$). This is because these expressions take into account the important fact that the presence of a reinforcement, with an expansion coefficient less than that of the matrix, introduces a mechanical constraint on the expansion of the matrix. A fiber will cause a greater constraint on the matrix than a particle. Let us consider the expansion coefficients of particulate and fibrous composites.

One can regard a particulate composite as a homogeneous material in a statistical sense, i.e., we assume a uniform distribution of the particles in the matrix. Let us denote the volume fractions of the two phases making a particulate composite by V_1

and V_2 (=1 − V_1). Various researchers have derived bounds and given expressions for the expansion coefficients and other transport properties such as thermal conductivity. Kerner (1956) developed the following expression for the volumetric expansion coefficient, β_c, of a composite consisting of spherical particles dispersed in a matrix:

$$\beta_c = \beta_m V_m + \beta_p V_p - (\beta_m - \beta_p) V_p \left[\frac{1/K_m - 1/K_p}{V_m/K_p + V_p/K_m + 0.75G_m} \right],$$

where subscripts c, m, and p denote the composite, matrix, and particle, respectively; β is the volumetric expansion coefficient, and K denotes the bulk modulus. Kerner's expression does not differ significantly from the rule-of-mixtures because the particle reinforcement constrains the matrix much less than fibers. The coefficient of linear thermal expansion according to Turner (1946) is given by:

$$\alpha_c = \frac{\alpha_m V_m K_m + \alpha_p V_p K_p}{V_p K_p + V_m K_m},$$

where the symbols have the significance given earlier. Turner's expression, generally, gives an expansion coefficient much lower than the rule-of-mixtures value.

Unidirectionally aligned fibrous composites have two (or sometimes three) thermal expansion coefficients: α_{cl} in the longitudinal direction and α_{ct} in the transverse direction. Fibers generally have a lower expansion coefficient than that of the matrix, and thus the fibers mechanically constrain the matrix. The constraint is more along the length of the fiber than in the radial direction. This results in the longitudinal coefficient of expansion of the composite, α_{cl} being smaller than the transverse coefficient, α_{ct} for the composite. At low fiber volume fractions, it is not unusual to find the transverse expansion of a fibrous composite, α_{ct}, greater than that of the matrix in isolation. The reason for this is as follows. The long, stiff, low CTE fibers prevent the matrix from expanding in the longitudinal direction, and as a result the matrix is forced to expand more than normal in the transverse direction. It should be pointed out that in the case of some CMCs, this situation can be reversed. For example, in the case of alumina fibers ($\alpha = 8 \times 10^{-6}\ \mathrm{K}^{-1}$) in a low-expansion glass or ceramic matrix, it is the matrix that will constrain the fibers, i.e., the situation in this case is the reverse of the one commonly encountered.

We give below some expressions for the CTE of unidirectionally reinforced fiber composites. All of these analyses involve the following assumptions:

1. The bonding between the fiber and matrix is perfect and mechanical in nature, i.e., no chemical interaction is allowed.
2. The fibers are continuous and perfectly aligned.
3. The properties of the constituents do not change with temperature.

Schapery (1969) used energy methods to derive the following expressions for expansion coefficient of a fibrous composite, assuming Poisson's ratios of the

components are not very different. The longitudinal expansion coefficient for the composite is

$$\alpha_{cl} = \frac{\alpha_m E_m V_m + \alpha_f E_f V_f}{E_m V_m + E_f V_f} \tag{10.38}$$

and the transverse expansion coefficient is

$$\begin{aligned} \alpha_{ct} &\simeq (1 + v_m)\alpha_m V_m + \left(1 + v_f\right)\alpha_f V_f - \alpha_{cl}\bar{v}, \\ \bar{v} &= v_f V_f + v_m V_m. \end{aligned} \tag{10.39a}$$

For high fiber volume fractions, $V_f > 0.2$ or 0.3, α_{ct} can be approximated by

$$\alpha_{ct} \simeq (1 + v_m)\alpha_m V_m + \alpha_f V_f. \tag{10.39b}$$

The longitudinal and transverse CTE for alumina fibers in an aluminum matrix are plotted in Fig. 10.7. Note the marked anisotropy in the expansion for aligned fibrous composites.

The anisotropy in expansion can be reduced somewhat if the composite contains randomly oriented short fibers or whiskers in three dimensions. We can write its isotropic thermal expansion coefficient

$$\alpha = \frac{\alpha_{cl} + 2\alpha_{ct}}{3}, \tag{10.40}$$

where α_{cl} and α_{ct} are given by Eqs. (10.38) and (10.39a, 10.39b).

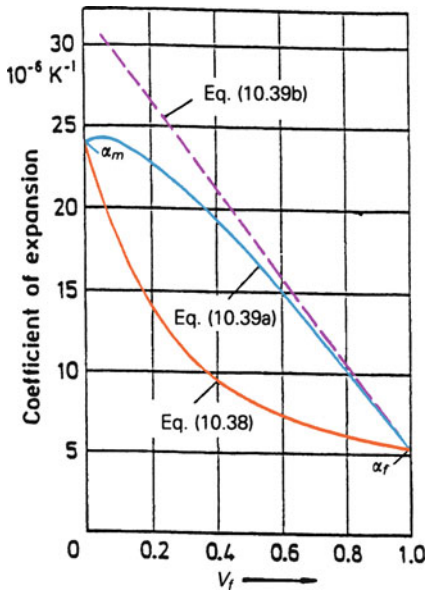

Fig. 10.7 Longitudinal and transverse linear thermal expansion coefficients vs. fiber volume fraction for alumina fiber in an aluminum matrix

It should be pointed out the length of fiber as well as fiber orientation has an effect on the CTEs (Marom and Weinberg 1975; Vaidya et al. 1994). It would appear that the fiber length has a more sensitive effect on the expansion characteristics because the constraint on the matrix is highest when the fibers are continuous. An extreme case of a low constraint is one of a matrix containing spherical particles, i.e., aspect ratio = 1. Continuous fibers with an aspect ratio of infinity represent the other extreme in constraint.

The effect of the fiber length on the thermal expansion can be incorporated into Schapery's equation as (Marom and Weinberg 1975; Vaidya and Chawla 1994)

$$\alpha_{11} = \frac{k\alpha_f V_f E_f + \alpha_m V_m E_m + \alpha_i V_i E_i}{kV_f E_f + V_m E_m + V_i E_i},$$

where the value of k is given by

$$k = \frac{l}{l_c} (l < l_c,\ 0 < k < 0.5),$$

$$k = 1 - l_c/2l (l > l_c,\ 0 < k < 1),$$

where l is the length and l_c is the critical length of the fiber (see Sect. 10.4).

Chamis (1983) used a simple force balance to arrive at the following expressions for α_1 and α_2:

$$\alpha_1 = \left[\frac{E_{f1}\alpha_{f1}V_f + E_m\alpha_m V_m}{E_{f1}V_f + E_m V_m}\right],$$

$$\alpha_2 = \alpha_{f2}\sqrt{V_f} + \left(1 - \sqrt{V_f}\right)\left(1 + V_f v_m \frac{E_{f1}}{E_c}\right)\alpha_m.$$

Rosen and Hashin (1970) used a plane strain model to derive expressions for α_1 and α_2:

$$\alpha_1 = \bar{\alpha} + \left[\frac{\alpha_f - \alpha_m}{1/K_f - 1/K_m}\right]\left[\frac{3(1 - 2v_c)}{E_c} - \frac{1}{K_c}\right],$$

$$\alpha_2 = \bar{\alpha} + \left[\frac{\alpha_f - \alpha_m}{1/K_f - 1/K_m}\right]\left[\frac{3}{2k_c} - \frac{3(1 - 2v_c)v_c}{E_c} - \frac{1}{K_c}\right],$$

where $\bar{\alpha} = \alpha_f V_f + \alpha_m V_m$, K_c is the composite bulk modulus, E_c is the composite Young's modulus, and k_c is the composite transverse bulk modulus.

Many applications of composites require controlled thermal expansion characteristics. All the expressions given above predict thermal expansion coefficients of composites based on continuum mechanics. That is, no account is taken of the effect of fiber or particle size on the CTE. Xu et al. (1994) examined the

effect of particle size on the CTE of TiC/Al XD™ composite, with two TiC particle sizes, 0.7 and 4 μm. The results of this work showed the effect of particle size on the thermal expansion coefficient of particle reinforced aluminum composites in terms of the degree of constraint on the matrix expansion. Careful TEM work showed lattice distortion at the interfacial zone. The effect of particle size on the CTE of composite was related to the volume fraction of interfacial zone through which the constraint occurs. A phenomenological approach that takes into account the different degree of constraint on the matrix expansion based on the TEM work allows us to compute the CTE of this composite with different particle sizes.

10.3.2 Expressions for Thermal Conductivity of Composites

Thermal conductivity is an important physical property. The heat flow in a material is proportional to the temperature gradient, and the constant of proportionality is called the *thermal conductivity*. Thus, in the most general form, using indicial notation, we can write

$$q_i = -k_{ij}\,\mathrm{d}T/\mathrm{d}x_j,$$

where q_i is the heat flux along the x_i axis, $\mathrm{d}T/\mathrm{d}x_j$ is the temperature gradient across a surface perpendicular to the x_j axis, and k_{ij} is the thermal conductivity. As should be evident from the two indexes, thermal conductivity is also a second-rank tensor. Although k_{ij} is not a symmetric tensor in the most general case, it is a symmetric tensor for most crystal systems. For an isotropic and a cubic material, k_{ij} reduces to a scalar number, k. For an orthotropic material, we have three constants along the three principal axes, viz., k_{11}, k_{22}, and k_{33}. For a transversely isotropic material such as a unidirectionally reinforced fibrous composite, there will be two constants: thermal conductivity in the axial direction, k_{cl}, and that in the transverse direction, k_{ct}. The thermal conductivity in the axial direction, k_{cl}, can be predicted by a rule-of-mixtures type expression (Behrens 1968)

$$k_1 = k_{cl} = k_{f1}V_f + k_m V_m, \tag{10.41}$$

where k_{f1} is the thermal conductivity of the fiber in the axial direction, k_m is that of the isotropic matrix, and V_f and V_m are the volume fractions of the fiber and matrix, respectively.

In a transverse direction, the thermal conductivity of a unidirectionally aligned fiber composite (i.e., transversely isotropic) can be approximated by the action-in-series model discussed earlier. This would give

$$k_{ct} = k_2 = k_{f2}k_m/\left(k_{f2}V_f + k_m V_m\right).$$

More complicated expressions have been derived for the transverse thermal conductivity. These expressions implicitly assume perfect contact between the fiber and the matrix. In real composites, it is likely that the thermal contact at the fiber/matrix interface will be less than perfect because of any microvoids, thermal mismatch, etc. An expression for the transverse thermal conductivity that takes into account the fact that the interface region may have a different thermal conductance than the matrix or the fiber is as follows (Hasselman and Johnson 1987):

$$\begin{aligned} k_{ct} = k_2 = k_m \big[\big(k_f/k_m - 1 - k_f/ah_{\mathrm{i}}\big)V_f \\ + \big(1 + k_f/k_m + k_f ah_{\mathrm{i}}\big)\big] \big/ \big[\big(1 - k_f/k_m + k_f/ah_{\mathrm{i}}\big)V_f \\ + \big(1 + k_f/k_m + k_f/ah_{\mathrm{i}}\big), \end{aligned} \tag{10.42}$$

where k_{m} is the matrix thermal conductivity, k_{f} is the transverse thermal conductivity of the fibers, V_{f} is the fiber volume fraction, a is the fiber radius, and h_{i} is the thermal conductance of the interface region. Note that the units of thermal conductivity are W/mK while for thermal conductance the units are W/K. The effect of interfacial conductivity is governed by the magnitude of nondimensional parameter, $k_{\mathrm{f}}/ah_{\mathrm{i}}$. h_{i} will have a value of infinity for perfect thermal contact and it will be equal to zero for a pore. Bhatt et al. (1992) studied the important role of interface in controlling the effective thermal conductivity of composites. In particular, one can use the measurement of thermal conductivity as a nondestructive tool to determine the integrity of the fiber/matrix interface.

We can also use Halpin-Tsai-Kardos equations to obtain the following expression for the transverse thermal conductivity of a composite containing unidirectionally aligned fibers:

$$k_{c2} = k_{c3} = k_{ct} = \big(1 + \eta V_f\big)\big/\big(1 - \eta V_f\big)k_m$$

and

$$\eta = [(k_{\mathrm{f}2}/k_m) - 1]/[(k_{\mathrm{f}2}/k_m) + 1],$$

where we have taken ζ equal to 1 in the Halpin-Tsai-Kardos equation.

Similar to the description of the coefficient of thermal expansion, we can find thermal conductivity of a unidirectionally reinforced fiber composite in any arbitrary direction if we know the thermal conductivity in directions 1 (longitudinal) and 2 (transverse). The thermal conductivity k_x and k_y in any arbitrary directions, x and y, respectively, are given by the following equations:

$$\begin{aligned} k_x &= k_1 \cos^2\theta + k_2 \sin^2\theta, \\ k_y &= k_1 \sin^2\theta + k_2 \cos^2\theta, \\ k_{xy} &= (k_2 - k_1)\sin\theta\cos\theta, \end{aligned}$$

Table 10.4 Thermal properties of a transversely isotropic composite (matrix isotropic, fiber anisotropic)

Heat capacity	$C = \frac{1}{\rho}(V_f \rho_f C_f + V_m \rho_m C_m)$
Longitudinal conductivity	$k_{11} = V_f k_{f1} + V_m k_m$
Transverse conductivity	$k_{22} = k_{33} = \left(1 - \sqrt{V_f}\right)k_m + \frac{k_m \sqrt{V_f}}{1 - \sqrt{V_f}(1 - k_m/k_{f2})}$
Longitudinal thermal expansion coefficient	$\alpha_{11} = \frac{V_f E_{f1} \alpha_{f1} + V_m E_m \alpha_m}{E_{f1} V_f + E_m V_m}$
Transverse thermal expansion coefficient	$\alpha_{22} = \alpha_{33} = \alpha_{f2}\sqrt{V_f} + \alpha_m\left(1 - \sqrt{V_f}\right)\left(1 + \frac{V_f \nu_m E_{f1}}{E_{f1} V_f + E_m V_m}\right)$

Source: Adapted with permission from Chamis (1983)

where θ is the angle between longitudinal (1) axis and the x axis, and k_{xy} can be considered to be a thermal coupling coefficient.

A summary of the general expressions for the thermal properties of a transversely isotropic fiber composite is given in Table 10.4.

Example 10.3 A unidirectional glass fiber reinforced epoxy has 50 vol.% of fiber. Estimate its thermal conductivity parallel to the fibers. Given $k_{glass} = 0.9$ W/mK, $k_{epoxy} = 0.15$ W/mK.

Solution Glass fiber is isotropic, i.e., $k_{f1} = k_{f2} = k_f$. The longitudinal thermal conductivity is given by

$$\begin{aligned} k_{ct} &= V_m k_m + V_f k_f \\ &= 0.5 \times 0.15 + 0.5 \times 0.9 \\ &= 0.075 + 0.45 = 0.525\,\text{W/mK}. \end{aligned}$$

Example 10.4 Derive an expression for the heat capacity, C_{pc}, of a composite.

Solution The total quantity of heat in the composite, Q_c, is the sum of heats in the fiber (Q_f) and matrix (Q_m). Thus,

$$Q_c = Q_f + Q_m.$$

The quantity of heat is heat capacity times the mass, i.e.,

$$Q_c = mC_p = v\rho C_{pc},$$

where m is the mass, v is the volume, ρ is the density, and C_{pc} is the heat capacity. Heat capacity is the amount of heat or thermal energy (J) required to raise the temperature of one mole of the maternal through one degree. It has the units of J/mol K. The specific heat of a material is the heat capacity per unit mass and it has the units of J/g K.

Using the subscripts c, f, and m for composite, fiber, and matrix, respectively, we can write

$$v_c \rho_c C_{pc} = v_f \rho_f C_{pf} + v_m \rho_m C_{pm}.$$

Remembering that $v_f/v_c = V_f$, the fiber volume fraction, and $v_m/v_c = V_m$, the matrix volume fraction, we can write

$$\rho_c C_{pc} = V_f \rho_f C_{pf} + V_m \rho_m C_{pm}$$

or

$$C_{pc} = \frac{1}{\rho_c [V_f \rho_f C_{pf} + V_m \rho_m C_{pm}].}$$

10.3.3 Electrical Conductivity

Electrical conductivity or its inverse electrical resistivity is another important physical property. In terms of electrical conductivity, composites represent a mixed bag. PMCs and CMCs are generally poor electrical conductors. The electrical conductivity of polymers can be increased by the addition of carbon fibers, carbon black, and graphite. Such composites can be used for situations involving electromagnetic and radio-frequency interference (EMI/RFI) shielding for electronic devices and for dissipation of static charge (Clingerman et al. 2002). Most metal matrix composites are mixtures of good electrical conductors (e.g., Cu, Al, etc.) and insulators (e.g., B, SiC, Al_2O_3, etc.), with W/Cu composite being a notable exception. We can write for the resistivity of a fiber reinforced composite in the axial direction a simple rule-of-mixtures type expression

$$\rho_{c\ell} = \rho_1 V_1 + \rho_2 V_2,$$

where ρ is the electrical resistivity, V is volume fraction, and the subscripts $c\ell$, 1, and 2 designate the composite in the longitudinal direction and the two components of the composite, respectively. Or in terms of electrical conductivity in the axial direction, σ, we can write

$$\sigma_{c\ell} = \sigma_1 V_1 + \sigma_2 V_2.$$

In the transverse direction, we have

$$\frac{1}{\sigma_{ct}} = \frac{V_1}{\sigma_1} + \frac{V_2}{\sigma_2},$$

where the symbols have the usual significance.

There is a logarithmic expression also

$$\log \sigma_c = V_1 \log \sigma_1 + V_2 \log \sigma_2.$$

Of course, one can generalize these expressions to more than two components in the composite, should that be the case.

Self-consistent models can also be used to get expressions for the electrical conductivity of a composite (Hale 1976).

The electrical resistivity (and therefore electrical conductivity) of the metal matrix in a composite is likely to be different from that of the unreinforced metal because of possible plastic deformation during processing which will introduce dislocations due to thermal mismatch between the matrix and the reinforcement; the dislocations in turn will increase the resistivity of the matrix. It should be pointed out that unlike the unreinforced metal, one cannot recover electrical conductivity by resorting to an annealing treatment. Physical properties such as thermal and electrical conductivity of composites depend on the properties of the matrix and reinforcement, their volume fractions, characteristics of the interface region, shape of the reinforcement, and the connectivity of the phases (Weber et al. 2003a, b; Weber 2005). The conductivity (thermal or electrical) of a composite will depend on conductivity characteristics of the matrix, reinforcement, volume fraction, and aspect ratio of the reinforcement, and, of course, the interfacial characteristics. In particular, interfacial resistance will vary with the form and size of reinforcement.

10.3.4 Hygral and Thermal Stresses

Hygroscopy, the ability of a substance to absorb water absorption, can be a problem with polymeric resins and natural fibers because it can lead to swelling. Swelling can lead to stresses if, as is likely in a composite, the material is not allowed to expand freely because of the presence of the matrix. Such stresses resulting from moisture absorption or hygroscopy are called *hygral stresses*. Thermal stresses will result in a material when the material is not allowed to expand or contract freely because of a constraint. When both hygral and thermal stresses are present, we call them *hygrothermal stresses*. Mathematically, these two types of internal stresses are quite similar, and we can treat them together.

Consider the passage of a composite from a reference state, where the body is stress-free and relaxed at a temperature T, concentration of moisture $C = 0$, and external stress $\sigma = 0$, to a final state where the body has hygrothermal as well as external stresses. We can consider that the final state of the composite with hygrothermal stresses and external loading is attained via two intermediate stages shown in Fig. 10.8. The final strain in the body can then be written as the sum of

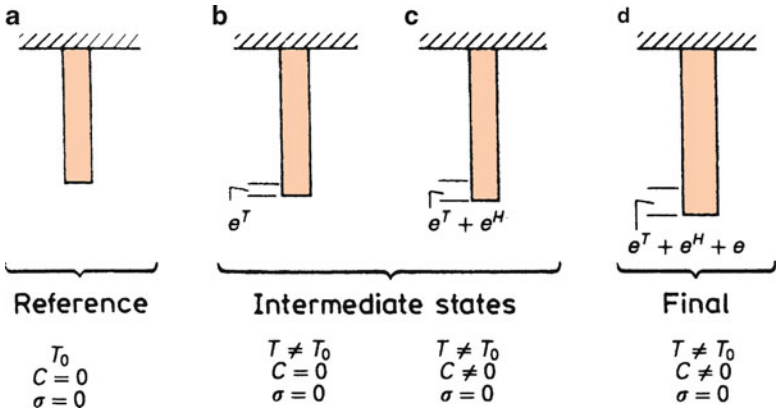

Fig. 10.8 (**a**) Strain-free reference state; (**b**) thermal strain (e^{T}); (**c**) hygral (e^{H}) and thermal (e^{T}) strains; and (**d**) final state: hygral (e^{H}), thermal (e^{T}), and mechanical strain

nonmechanical (thermal strain, e_i^{T} and hygral strain, e_i^{H}) and mechanical strains. The mechanical strain is given by the Hooke's law (compliance times the stress). Thus,

$$e_t = \underbrace{e_i^{\mathrm{T}} + e_i^{\mathrm{H}}}_{\text{nonmechanical strains}} + \underbrace{S_{ij}\sigma_j}_{\text{mechanical strain}}, \tag{10.43}$$

where S_{ij} is the compliance. If we regard the composite as transversely isotropic, we can immediately write the following relationships for the strain components

$$\begin{gathered} e_{xy}^{\mathrm{T}} = e_{xy}^{\mathrm{H}} = 0, \\ e_y^{\mathrm{T}} = e_z^{\mathrm{T}} \quad \text{and} \quad e_y^{\mathrm{H}} = e_z^{\mathrm{H}}, \\ e_i^{\mathrm{T}} = \alpha_i (T - T_0), \\ e_i^{\mathrm{H}} = \beta_i C, \end{gathered} \tag{10.44}$$

where the α_i are thermal expansion coefficients (K^{-1}), the β_i are nondimensional swelling coefficients, T is the temperature, T_0 is the equilibrium temperature, C is the concentration of water vapor, and the superscripts H and T indicate hygral and thermal strain components, respectively.

Total volumetric hygrothermal strain can be expressed as the sum of the diagonal terms of the strain matrix. It is important to note that the thermal and hygral effects are dilational only, i.e., they cause only expansion or contraction but do not affect the shear components. Thus,

$$\begin{aligned} \frac{\Delta V}{V} &= e_x^{\mathrm{T}} + e_y^{\mathrm{T}} + e_z^{\mathrm{T}} + e_x^{\mathrm{H}} + e_y^{\mathrm{H}} + e_z^{\mathrm{H}} \\ &= e_x^{\mathrm{T}} + 2e_y^{\mathrm{T}} + e_x^{\mathrm{H}} + 2e_y^{\mathrm{H}}. \end{aligned} \tag{10.45}$$

Hygrothermal stresses are very important in polymer matrix composites (see also Chaps. 3 and 5).

We first consider the constitutive equations for an isotropic material and then for an anisotropic material. Consider an isotropic material, in plane stress, subjected to a temperature change, ΔT, and a change in moisture content, ΔC. We can write the constitutive equations for this case as follows

$$\varepsilon_1 = \sigma_1/E - \nu\sigma_2/E + \beta\Delta C + \alpha\Delta T,$$
$$\varepsilon_2 = \nu\sigma_1/E - \sigma_2/E + \beta\Delta C + \alpha\Delta T,$$
$$\varepsilon_6 = \sigma_6/G.$$

Note that, as pointed out earlier, ΔC and ΔT do not produce shear strains. For a specially orthotropic, unidirectionally reinforced fiber lamina (i.e., one in which material and geometric axes coincide, see also Chap. 11), we can write

$$\begin{bmatrix}\varepsilon_1\\ \varepsilon_2\\ \varepsilon_6\end{bmatrix} = \begin{bmatrix}S_{11} & S_{12} & 0\\ & S_{22} & 0\\ & & S_{66}\end{bmatrix}\begin{bmatrix}\sigma_1\\ \sigma_2\\ \sigma_6\end{bmatrix} + \begin{bmatrix}\alpha_1\\ \alpha_2\\ 0\end{bmatrix}\Delta C + \begin{bmatrix}\beta_1\\ \beta_2\\ 0\end{bmatrix}\Delta T.$$

In this expression the subscript 6 indicate inplane shear. We explain this notation in Chap. 11. In a PMC, the matrix is likely to absorb more moisture than the fiber, which will lead to $\beta_2 > \beta_1$. In an off-axis, generally orthotropic, unidirectionally reinforced fiber lamina, the material and geometric axes do not coincide, and the strain components take the following form

$$\begin{bmatrix}\varepsilon_x\\ \varepsilon_y\\ \varepsilon_s\end{bmatrix} = \begin{bmatrix}\overline{S_{11}} & \overline{S_{12}} & \overline{S_{16}}\\ & \overline{S_{22}} & \overline{S_{26}}\\ & & \overline{S_{66}}\end{bmatrix}\begin{bmatrix}\sigma_x\\ \sigma_y\\ \sigma_s\end{bmatrix} + \begin{bmatrix}\alpha_x\\ \alpha_y\\ \alpha_s\end{bmatrix}\Delta C + \begin{bmatrix}\beta_x\\ \beta_y\\ \beta_s\end{bmatrix}\Delta T,$$

where $\bar{S}_{ij}$ designate the compliance matrix for the generally orthotropic lamina.

10.3.5 Thermal Stresses in Fiber Reinforced Composites

During curing or solidification of the matrix around reinforcement fibers or particles, a large magnitude of shrinkage stresses can result. The interfacial pressure developed during curing is akin to that obtained upon embedding a cylinder (sphere) of radius $r + \delta r$ in a cylindrical (spherical) hole of radius r. The thermal stresses generated depend on the reinforcement volume fraction, reinforcement geometry, thermal mismatch ($\Delta\alpha$), and the modulus ratio, E_r/E_m where E is the Young's modulus and the subscripts r and m refer to the reinforcement and matrix, respectively. Generally, $\alpha_m > \alpha_f$; that is, on cooling from T_0 to T ($T_0 > T$), the matrix would tend to contract more than the fibers, causing the fibers to experience axial compression. In extreme cases, fiber buckling can also lead to the generation of interfacial shear stresses. This problem of thermal stresses in composite materials is a most serious and important problem. It is worth repeating that thermal stresses

are internal stresses that arise whenever there is a constraint on the free dimensional change of a body (Chawla 1973a). In the absence of this constraint, the body can experience free thermal strains without any accompanying thermal stresses. The constraint can have its origin in (1) a temperature gradient, (2) crystal structure anisotropy (e.g., a noncubic structure), (3) phase transformations resulting in a volume change, and (4) a composite material made of dissimilar materials (i.e., materials having different CTEs). The thermal gradient problem is a serious one in ceramic materials in general. A thermal gradient ΔT is inversely related to the thermal diffusivity, a, of a material. Thus,

$$\Delta T = \phi\left(\frac{1}{a}\right) = \phi\left(\frac{C_p p}{k}\right), \tag{10.46}$$

where C_p is the specific heat, ρ is the density, and k is the thermal conductivity. Metals generally have high thermal diffusivity and any thermal gradients that might develop are dissipated rather quickly. It should be emphasized that in composite materials even a uniform temperature change (i.e., no temperature gradient) will result in thermal stresses owing to the ever-present thermal mismatch (Chawla 1973a). Thermal stresses resulting from a thermal mismatch will generally have an expression of the form

$$\sigma = f(E\Delta\alpha\Delta T). \tag{10.47}$$

We describe below first the three-dimensional thermal stress state in a composite consisting of a central fiber surrounded by its shell of matrix; see Fig. 10.5. After this, we derive the three-dimensional stress state for a particulate composite.

The elasticity problem is basically the same as the one discussed for transverse stresses (see Sect. 10.2.4). We use polar coordinates; r, θ, and z (see Fig. 10.5). Axial symmetry makes shear stresses go to zero and the principal stresses are independent of θ. At low volume fractions, the outer cylinder is the matrix and the inner cylinder is the fiber. The expressions for strain in the generalized Hooke's law contain an $\alpha\Delta T$ term. Thus, for component 2,

$$\begin{aligned}
e_{r2} &= \frac{\sigma_{r2}}{E_2} - \frac{\nu_2}{E_2}(\sigma_{\theta 2} + \sigma_{z2}) + \alpha_2 \Delta T \\
e_{\theta 2} &= \frac{\sigma_{\theta 2}}{E_2} - \frac{\nu_2}{E_2}(\sigma_{r2} + \sigma_{z2}) + \alpha_2 \Delta T \\
e_{z2} &= \frac{\sigma_{z2}}{E_2} - \frac{\nu_2}{E_2}(\sigma_{r2} + \sigma_{\theta 2}) + \alpha_2 \Delta T
\end{aligned}$$

The resultant stresses in 1 and 2 will have the form (see Sect. 10.2.4)

$$\begin{array}{ll}
\text{Component 1} & \text{Component 2} \\
\sigma_{r1} = A_1 & \sigma_{r2} = A_2 - \dfrac{B_2}{r^2} \\
\sigma_{\theta 1} = A_1 & \sigma_{\theta 2} = A_2 + \dfrac{B_2}{r^2} \\
\sigma_{z1} = C_1 & \sigma_{z2} = C_2
\end{array} \tag{10.48}$$

The following boundary conditions exist for our problem:

1. At the interface $r = a$, $\sigma_{r1} = \sigma_{r2}$ for stress continuity.
2. At the free surface $r = b$, $\sigma_{r2} = 0$.
3. The resultant of axial stress σ_z on a section $z =$ constant is zero.
4. Radial displacements in the two components are equal at the interface; that is, at $r = a$, $u_{r1} = u_{r2}$.
5. The radial displacement in component 1 must vanish at the symmetry axis; that is, at $r = 0$, $u_{r1} = 0$.

Using these boundary conditions, it is possible to determine the constants given in Eq. (10.48). The final equations for the matrix sleeve are given here (Poritsky 1934; Chawla 1973b):

$$\sigma_r = A\left(1 - \frac{b^2}{r^2}\right), \qquad \sigma_\theta = A\left(1 + \frac{b^2}{r^2}\right), \qquad \sigma_z = B, \tag{10.49}$$

where

$$A = -\left[\frac{E_m(\alpha_m - \alpha_f)\Delta T(a/b)^2}{1 + (a/b)^2(1 - 2v)\left[(b/a)^2 - 1\right]E_m/E_f}\right],$$

$$B = \frac{A}{(a/b)^2} \times \left[2v\left(\frac{a}{b}\right)^2 + \frac{1 + (a/b)^2(1 - 2v) + (a/b)^2(1 - 2v)\left[(b/a)^2 - 1\right]E_m/E_f}{1 + \left[(b/a)^2 - 1\right]E_m/E_f}\right].$$

$$v_m = v_f = v$$

A plot of σ_r, σ_θ, and σ_z against r/a, where r is the distance in the radial direction and a is the fiber radius, is shown in Fig. 10.9 for the system W/Cu for two fiber volume fractions (Chawla and Metzger 1972). Note the change in stress level of σ_z with V_f. This thermoelastic solution can provide information about the magnitude of the elastic stresses involved. A comparison with the yield or fracture strength of the matrix can inform us whether or not plastic deformation or fracture of matrix will occur. Also, if the matrix deforms plastically in response to these thermal stresses, the plots of thermal stress distribution can tell where the plastic deformation will begin. Chawla and Metzger (1972) and Chawla (1973a, b, 1974, 1976a, b), in a series of studies with metal matrix composites, showed that the magnitude of the thermal stresses generated is large enough to deform the soft metallic matrix plastically. Depending on the temperatures involved, the plastic deformation of the metal matrix could involve slip, cavitation, grain boundary sliding, and/or migration. They measured the dislocation densities in the copper matrix of tungsten filament/copper single-crystal composites by the etch-pitting technique and showed

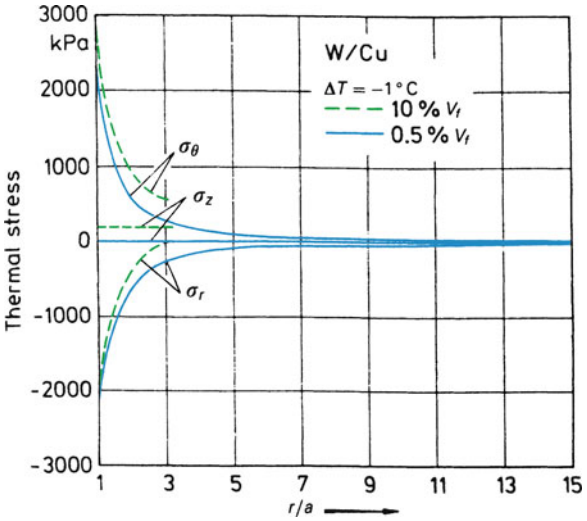

Fig. 10.9 Three-dimensional thermal stress state in a tungsten fiber/copper matrix composite for two different volume fractions. Note the change in σ_z level with V_f [from Chawla and Metzger (1972), used with permission]

that the dislocation densities were higher near the fiber/matrix interface than away from the interface, indicating that the plastic deformation, in response to thermal stresses, initiated at the interface. Figure 10.10 shows the variation of dislocation density (≃etch pit density) vs. distance from the interface. The increase in the dislocation density in the plateau region with V_f (in Fig. 10.10) is due to a higher σ_z with higher V_f value (see Fig. 10.9). Tresca or von Mises yield criteria applied to the stress situation shown in Fig. 10.9 will indicate that the matrix plastic flow starts at the interface. Dislocation generation due to thermal mismatch between reinforcement and a metallic matrix has been observed in TEM by many researchers (e.g., Arsenault and Fisher 1983; Vogelsang et al. 1986); see Fig. 10.11a. In the case of a fiber reinforced CMC, the ceramic matrix is unlikely to undergo plastic deformation; it is more likely to suffer microcracking as a result of thermal stresses. As an example of this, consider a composite made of $CaTiO_3$ and Al_2O_3. The laminated composite was made by hot pressing of these two ceramic components, which involved a cool down of about 1,000 °C. Such a temperature excursion would result in tensile stress in $CaTiO_3$ because $CaTiO_3$ has a larger CTE (13×10^{-6} K^{-1}) compared to Al_2O_3 (8×10^{-6} K^{-1}). The magnitude of tensile stress is large enough to cause cracks in $CaTiO_3$ during cool down after hot pressing; see the cracks in the $CaTiO_3$ layer in Fig. 10.11b (Gladysz and Chawla 2001).

10.3.6 Thermal Stresses in Particulate Composites

The particulate form of reinforcement can result in a considerably reduced degree of anisotropy. However, so long as a thermal mismatch exists between the particle and the matrix, thermal stresses will be present in such composites as well. Consider a particulate composite consisting of small particles distributed in a

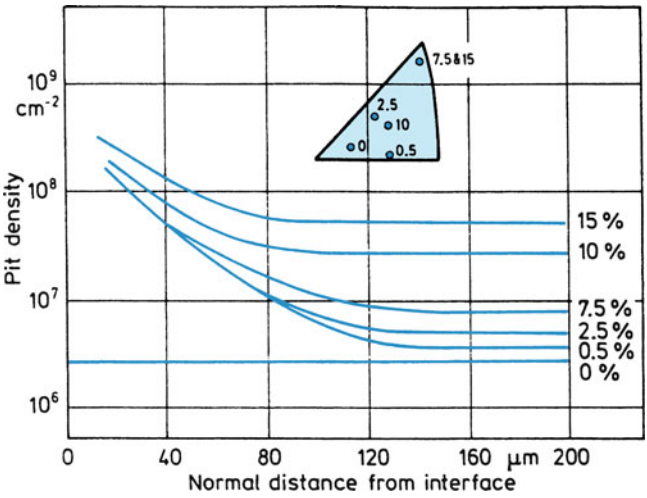

Fig. 10.10 Variation of dislocation density (≃pit density) with distance from the interface. The higher dislocation density in the plateau region with high V_f is due to a higher σ_z with higher V_f (Fig. 10.9) [from Chawla and Metzger (1972), used with permission]

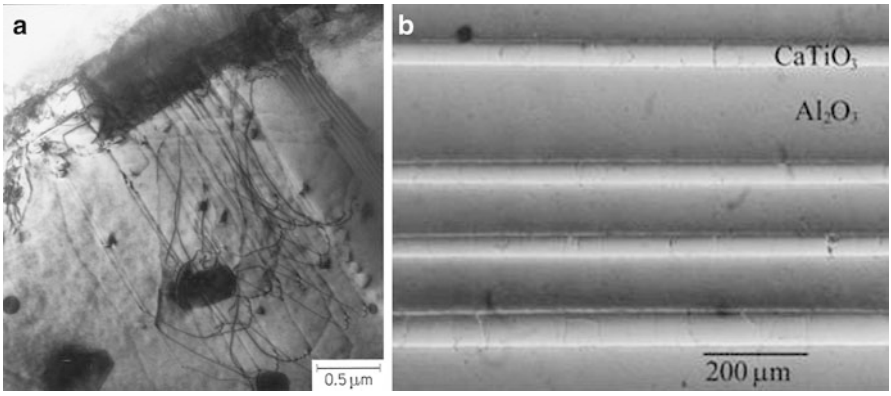

Fig. 10.11 (**a**) Dislocations generated at SiC whiskers in an aluminum matrix in an in situ thermal cycling experiment done in a high-voltage electron microscope [from Vogelsang et al. (1986), used with permission]. (**b**) Cracking in the $CaTiO_3$ layer in a $CaTiO_3/Al_2O_3$ composite due to thermal stresses generated during cool down from the processing temperature (from Gladysz and Chawla 2001)

matrix. If we regard this composite as an assembly of elastic spheres of uniform size embedded in an infinite elastic continuum, then it can be shown from the theory of elasticity (see, for example, Timoshenko and Goodier 1951) that an axially symmetrical stress distribution will result around each particle. Figure 10.12 shows a schematic of such a particle reinforced composite. The particle radius is a while the

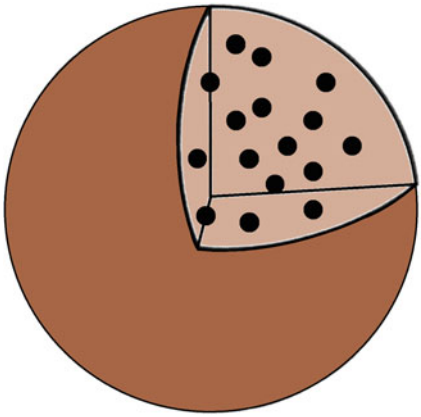

Fig. 10.12 A particle reinforced composite

surrounding matrix sphere has a radius b. This elasticity problem has spherical symmetry, therefore the use of spherical coordinates, r, θ, and ϕ as indicated in Fig. 10.13a makes for a simple analysis. We have the following components of stress, σ, strain, ε, and displacement, u:

$$\sigma_r, \sigma_\theta = \sigma_\phi,$$

$$\varepsilon_r, \varepsilon_\theta = \varepsilon_\phi,$$

$$u_r = u, \quad \text{independent of } \theta \text{ or } \phi.$$

The equilibrium equation for this spherically symmetric problem is

$$\frac{\mathrm{d}\sigma_r}{\mathrm{d}r} + \frac{2}{r}(\sigma_r - \sigma_\theta) = 0 \tag{10.50}$$

while the strain–displacement relationships are

$$\varepsilon_r = \frac{\mathrm{d}u}{\mathrm{d}r}, \qquad \varepsilon_\theta = \frac{u}{r}. \tag{10.51}$$

Substituting Eq. (10.51) in Eq. (10.50), we get the governing differential equation for our problem:

$$\frac{d^2u}{dr^2} + \frac{2}{r}\frac{du}{dr} - \frac{2}{r^2}u = 0 \tag{10.52}$$

The solution to this differential equation is

$$u = Ar + \frac{C}{r^2}.$$

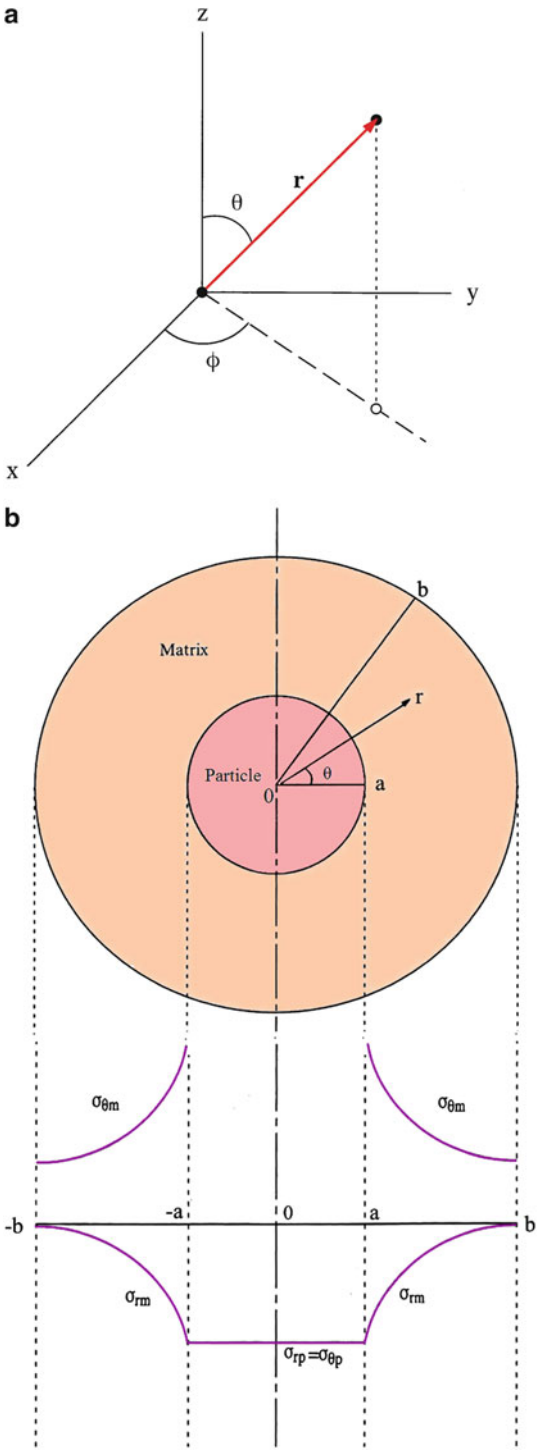

Fig. 10.13 (**a**) Spherical coordinate system. (**b**) Stress distribution in a particulate composite for cool down from the processing temperature

We apply the following boundary conditions:

1. Stress vanishes at the free surface (i.e., at $r = b$).
2. The radial stress at the interface ($r = a$) is the interfacial pressure, P, i.e.,

$$\sigma_r(a) = -P$$

The particle has a hydrostatic state of stress with the stress components

$$\sigma_{rp} = -P = \text{constant} = \sigma_{\theta p} \tag{10.53}$$

while the stresses in the matrix are

$$\sigma_{rm} = \frac{P}{1 - V_p}\left[\frac{a^3}{r^3} - V_p\right], \tag{10.54}$$

$$\sigma_{\theta m} = -\frac{P}{1 - V_p}\left[\frac{1}{2}\frac{a^3}{r^3} + V_p\right], \tag{10.55}$$

$$P = \frac{(\alpha_m - \alpha_p)\Delta T}{\left[\dfrac{0.5(1 + \nu_m) + (1 - 2\nu_m)V_p}{E_m(1 - V_p)} + \dfrac{1 - 2\nu_p}{E_p}\right]}, \tag{10.56}$$

$$V_p = \left(\frac{a}{b}\right)^3,$$

where V_p is the particle volume fraction, a is the particle radius, b is the matrix radius, and other symbols have the significance given earlier. Figure 10.13b shows the stress distribution in a particulate composite when cooled down from the processing temperature and for $\alpha_m > \alpha_p$. Note the different stress distribution in a particulate composite from that in a fibrous composite. The particle is under a uniform pressure, P, while the matrix has different radial and tangential stress components. The radial and tangential components in the matrix vary with distance, as shown in Fig. 10.13b. The radial component goes to zero at the free surface, $r = b$, as per our boundary conditions. The tangential component has a nonzero value at the free surface.

10.4 Mechanics of Load Transfer from Matrix to Fiber

The topic of load transfer from the matrix to the fiber has been treated by a number of researchers (Cox 1952; Dow 1963; Schuster and Scala 1964; Kelly 1973). The matrix holds the fibers together and transmits the applied load to the fibers, the real load-bearing component in most cases. Let us focus our attention on a high-

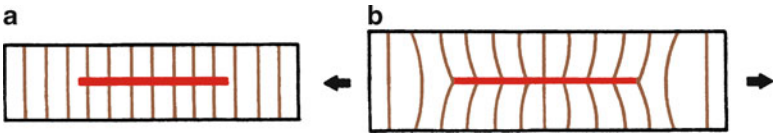

Fig. 10.14 A high-modulus fiber embedded in a low-modulus matrix: (**a**) before deformation, (**b**) after deformation

modulus fiber embedded in a low-modulus matrix. Figure 10.14a shows the situation prior to the application of an external load. We assume that the fiber and matrix are perfectly bonded and that the Poisson's ratios of the two are the same. Imagine vertical lines running through the fiber/matrix interface in a continuous manner in the unstressed state, as shown in Fig. 10.14a. Now let us load this composite axially as shown in Fig. 10.14b. We assume that no direct loading of the fibers occurs. Then the fiber and the matrix experience locally different axial displacements because of the different elastic moduli of the components. Different axial displacements in the fiber and the matrix mean that shear strains are being produced in the matrix on planes parallel to the fiber axis and in a direction parallel to the fiber axis. Under such circumstances, our imaginary vertical lines of the unstressed state will become distorted, as shown in Fig. 10.14b. Transfer of the applied load to the fiber thus occurs by means of these shear strains in the matrix. Termonia (1987) used a finite difference numerical technique to model the elastic strain field perturbance in composite consisting of an embedded fiber in a matrix when a uniform far field strain was imposed on the matrix. An originally uniform orthogonal mesh around the fiber became distorted when an axial tensile stress was applied.

It is instructive to examine the stress distribution along the fiber/matrix interface. There are two important cases: (1) both the matrix and fiber are elastic, and (2) the matrix is plastic and the fiber is elastic. Fibers such as boron, carbon, and ceramic fibers are essentially elastic right up to fracture. Metallic matrices show elastic and plastic deformation before fracture, while thermoset polymeric and ceramic matrices can be treated, for all practical purposes, as elastic up to fracture.

10.4.1 Fiber Elastic–Matrix Elastic

Consider a fiber of length l embedded in a matrix subjected to a strain; see Fig. 10.15. We assume that (1) there exists a perfect bonding between the fiber and matrix (i.e., there is no sliding between them) and (2) the Poisson's ratios of the fiber and matrix are equal, which implies an absence of transverse stresses when the load is applied along the fiber direction. Let the displacement of a point at a distance x from one extremity of the fiber be u in the presence of a fiber and v in the absence of a fiber. Then we can write for the transfer of load from the matrix to the fiber

$$\frac{\mathrm{d}P_f}{\mathrm{d}x} = B(u - v), \tag{10.57}$$

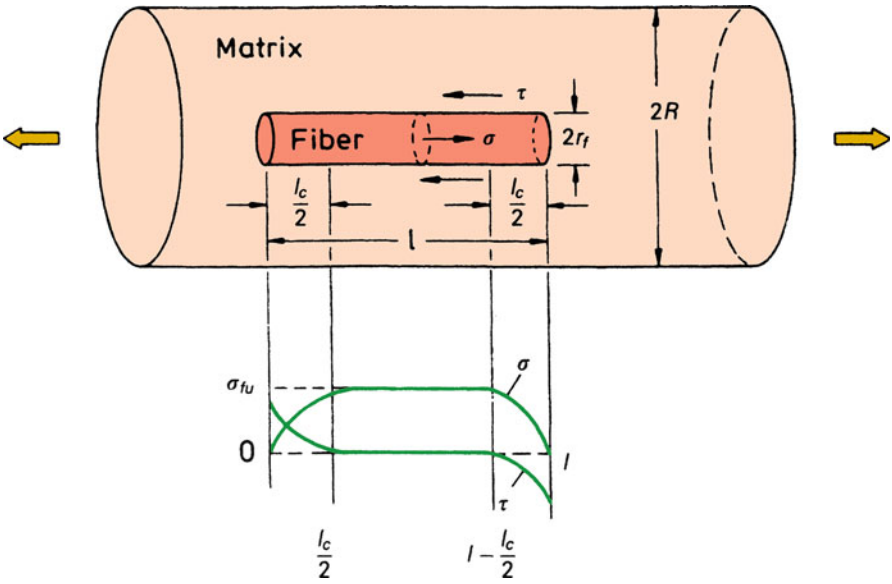

Fig. 10.15 Load transfer in a fiber/matrix composite and variation of tensile stress (σ_f) in the fiber and interfacial shear stress (τ) with distance along the interface

where P_f is the load on the fiber and B is a constant that depends on the geometric arrangement of fibers, the matrix type, and moduli of the fiber and matrix. Differentiating Eq. (10.57), we get

$$\frac{d^2P_f}{dx^2} = B\left(\frac{du}{dx} - \frac{dv}{dx}\right). \tag{10.58}$$

We have

$$\frac{du}{dx} = \text{strain in fiber} = \frac{P_f}{E_f A_f},$$

$$\frac{dv}{dx} = \text{strain in the matrix away from the fiber}$$

$$= \text{imposed strain}, e.$$

Thus, Eq. (10.58) can be rewritten as

$$\frac{d^2P_f}{dx^2} = B\left(\frac{P_f}{A_f E_f} - e\right). \tag{10.59}$$

A solution of this differential equation is

$$P_f = E_f A_f e + S \sinh \beta x + T \cosh \beta x, \tag{10.60}$$

where S and T are constants of integration and

$$\beta = \left(\frac{B}{A_f E_f} \right)^{1/2}. \tag{10.61}$$

We use the following boundary condition to evaluate the constants S and T:

$$P_f = 0 \text{ at } x = 0 \text{ and } x = l.$$

Putting in these values and using the half-angle trigonometric formulas, we get the following result:

$$P_f = E_f A_f e \left[1 - \frac{\cosh \beta (l/2 - x)}{\cosh(\beta l/2)} \right] \quad \text{for} \quad 0 < x < l/2 \tag{10.62}$$

or

$$\sigma_f = \frac{P_f}{A_f} = E_f e \left[1 - \frac{\cosh \beta (l/2 - x)}{\cosh(\beta l/2)} \right] \quad \text{for} \quad 0 < x < l/2. \tag{10.63}$$

The maximum possible value of strain in the fiber is the imposed strain e, and thus the maximum stress is $E_f e$. Therefore, if we have a long enough fiber, the stress in the fiber will increase from the two ends to a maximum value, $\sigma_{fu} = E_f e$. It can be shown readily that the average stress in the fiber is

$$\overline{\sigma}_f = \frac{E_f e}{l} \int_0^l \left[1 - \frac{\cosh \beta (l/2 - x)}{\cosh(\beta l/2)} \right] \mathrm{d}x = E_f e \left[1 - \frac{\tanh(\beta l/2)}{\beta l/2} \right]. \tag{10.64}$$

We can obtain the variation of shear stress τ along the fiber/matrix interface by considering the equilibrium of forces acting over an element of fiber (radius r_f). Thus, from Fig. 10.15 we can write

$$\frac{\mathrm{d}P_f}{\mathrm{d}x} \mathrm{d}x = 2\pi r_f \, \mathrm{d}x \, \tau. \tag{10.65}$$

Now P_f, the tensile load on the fiber, is equal to $\pi r_f^2 \sigma_f$. Substituting this in Eq. (10.65), we get

$$\tau = \frac{1}{2\pi r_f} \frac{\mathrm{d}P_f}{\mathrm{d}x} = \frac{r_f}{2} \frac{\mathrm{d}\sigma_f}{\mathrm{d}x}. \tag{10.66}$$

From Eqs. (10.63) and (10.66), we obtain

$$\tau = \frac{E_f r_f e\beta}{2} \frac{\sinh \beta(l/2 - x)}{\cosh(\beta l/2)}. \tag{10.67}$$

Figure 10.15 shows the variation of τ and σ_f with distance x. The maximum shear stress, in Eq. (10.67), will be the smaller of the following two shear strength values: (1) the shear yield strength of the matrix or (2) the shear strength of the fiber/matrix interface. Whichever of these two shear strength values is attained first will control the load transfer phenomenon and should be used in Eq. (10.67).

Now we can determine the constant B. The value of B depends on the fiber packing geometry. Consider Fig. 10.15 again and let the fiber length l be much greater than the fiber radius r_f. Let $2R$ be the average fiber spacing (center to center). Let us also denote the shear stress in the fiber direction at a distance r from the axis by $\tau(r)$. Then, at the fiber surface ($r = r_f$), we can write

$$\frac{dP_f}{dx} = -2\pi r_f \tau(r_f) = B(u - v).$$

Thus,

$$B = -\frac{2\pi r_f \tau(r_f)}{u - v}. \tag{10.68}$$

Let w be the real displacement in the matrix. Then at the fiber/matrix interface, no sliding being permitted, $w = u$. At a distance R from the center of a fiber, the matrix displacement is unaffected by the fiber presence and $w = v$. From the equilibrium of forces acting on the matrix volume between r_f and R, we can write

$$2\pi r\tau(r) = \text{constant} = 2\pi r_f \tau(r_f),$$

or

$$\tau(r) = \frac{\tau(r_f) r_f}{r}. \tag{10.69}$$

The shear strain γ in the matrix is given by $\tau(r) = G_m \gamma$, where G_m is the matrix shear modulus. Then

$$\gamma = \frac{dw}{dr} = \frac{\tau(r)}{G_m} = \frac{\tau(r_f) r_f}{G_m r}. \tag{10.70}$$

Integrating from r_f to R, we obtain

$$\int_{r_f}^{R} \mathrm{d}w = \Delta w = \frac{\tau(r_f) r_f}{G_m} \int_{r_f}^{R} \frac{1}{r} \mathrm{d}r = \frac{\tau(r_f) r_f}{G_m} \ln\left(\frac{R}{r_f}\right). \tag{10.71}$$

But, by definition,

$$\Delta w = v - u = -(u - v). \tag{10.72}$$

From (10.71) and (10.72), we get

$$\frac{\tau(r_f) r_f}{u - v} = -\frac{G_m}{\ln(R/r_f)}. \tag{10.73}$$

From Eqs. (10.68) and (10.73), one obtains

$$B = \frac{2\pi G_m}{\ln(R/r_f)} \tag{10.74}$$

and from Eq. (10.61), one can obtain an expression for the load transfer parameter β:

$$\beta = \left(\frac{B}{E_f A_f}\right)^{1/2} = \left[\frac{2\pi G_m}{E_f A_f \ln(R/r_f)}\right]^{1/2}. \tag{10.75}$$

The value of R/r_f is a function of fiber packing. For a square array of fibers, we have $\ln(R/r_f) = \frac{1}{2}\ln(\pi/V_f)$. For a hexagonal packing of fibers, we have $\ln(R/r_f) = \frac{1}{2}\ln(2\pi/\sqrt{3}V_f)$. We can define $\ln(R/r_f) = \frac{1}{2}\ln(\phi_{\max}/V_f),$, where $\phi_{\max}$ is the maximum packing factor. Substituting this in Eq. (10.75), we get

$$\beta = \left[\frac{4\pi G_m}{E_f A_f \ln(\phi_{\max}/V_f)}\right]^{1/2}.$$

Note that the greater the value of the ratio $G_\mathrm{m}/E_\mathrm{f}$, the greater the value of β and the more rapid the stress increase in the fiber from either end.

More rigorous analyses give results similar to the one above and differ only in the value of β. In all analyses, β is proportional to $(G_\mathrm{m}/E_\mathrm{f})^{1/2}$, and differences occur only in the term involving fiber volume fraction, $\ln(R/r_\mathrm{f})$, in the preceding equation.

Termonia (1987) used the finite difference method to show the high shear strains in the matrix near the fiber extremeties. Micro-Raman spectroscopy has been used to study the deformation behavior of organic and inorganic fiber reinforced composites (Galiotis et al. 1985; Day et al. 1987, 1989; Schadler and Galiotis 1995; Yang et al. 1992; Young et al. 1990). Characteristic Raman spectra can be obtained from these fibers in the undeformed and the deformed states. Under tension, the peaks of the Raman bands shift to lower frequencies. The magnitude of

frequency shift is a function of the material, Raman band under consideration, and the Young's modulus of the material. The shift in Raman bands results from changes in force constants due to changes in molecular or atomic bond lengths and bond angles. Micro-Raman spectroscopy is a very powerful technique that allows us to obtain point-to-point variation in strain along the fiber length embedded in a transparent matrix. An example of this for Kevlar aramid 149/epoxy composite is shown in Fig. 10.16 (Young 1994). In Fig. 10.16a, b, we see that up to 1 % strain, the strain in the fiber builds from the two ends as predicted by the shear lag analysis described earlier, while in the middle of the fiber length the strain in the fiber and matrix are equal. In Fig. 10.16c, d, we see that as fiber fractures at different sites along its length, the strain in fiber drops at those sites.

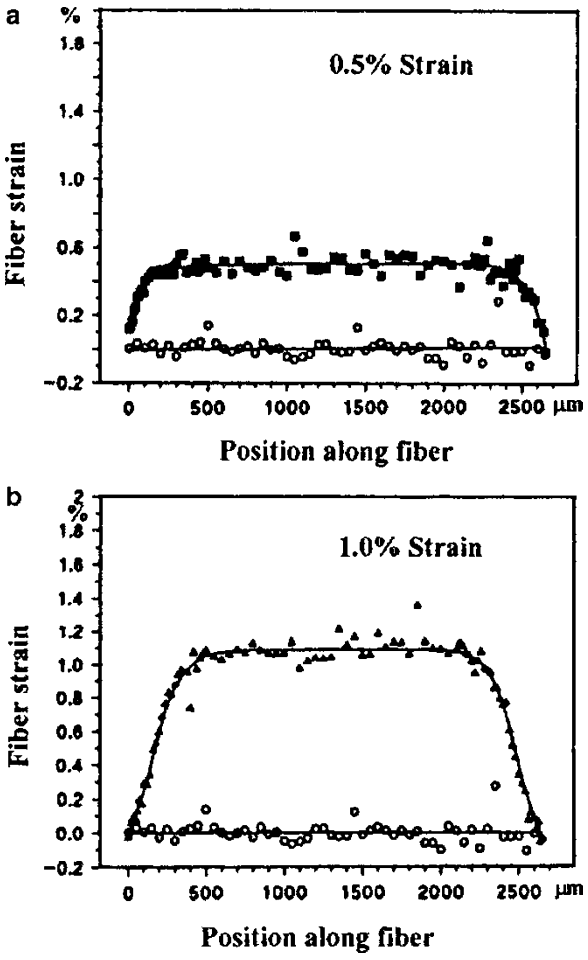

Fig. 10.16 Micro-Raman spectra of Kevlar aramid 149 when the Kevlar/epoxy composite is loaded axially. (**a**, **b**) Strain build up in the fiber from the two ends. (**c**, **d**) Fiber fracture leads to a drop in strain at those sites [after Young (1994)]

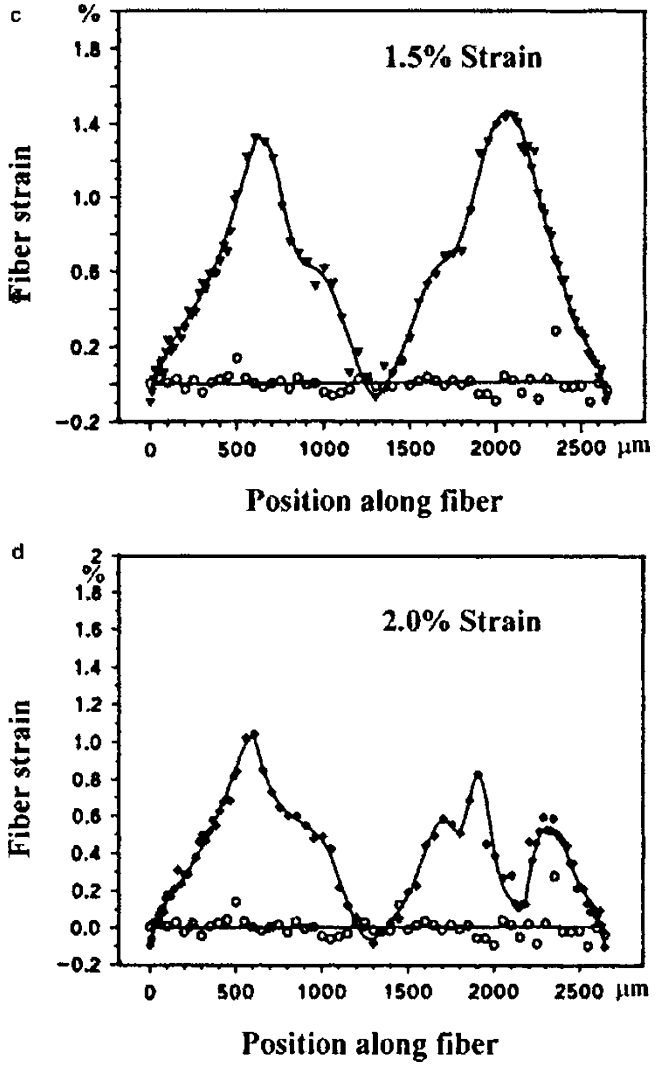

Fig. 10.16 (continued)

Let us reexamine Fig. 10.15. As per our boundary condition, the normal stress is zero at the two extremities of the fiber. The normal stress, σ, rises from the two ends to a maximum value along most of the fiber length, provided we have a long enough fiber. This gives rise to the concept of a critical fiber length for load transfer (see the next section). The shear stress is maximum at the fiber ends. Matrix yielding or interfacial failure would be expected to start at the fiber ends.

10.4.2 Fiber Elastic–Matrix Plastic

It should be clear from the preceding discussion that in order to load high-strength fibers in a ductile matrix to their maximum strength, the matrix shear strength must be large. A metallic matrix will flow plastically in response to the high shear stresses developed. Of course, if the shear strength fiber/matrix interface is less than the shear yield strength of the matrix, then the interface will fail first. In MMCs, assuming that the plastically deforming matrix does not work-harden, the shear stress at the fiber surface, $\tau(r_f)$, will have an upper limit of τ_y, the matrix shear yield strength. In PMCs and CMCs, frictional slip at the interface is more likely than plastic flow of the matrix. In the case of PMCs and CMCs, therefore, the limiting shear stress will be the interface strength in shear, τ_i. The term τ_i should replace τ_y in what follows for PMCs and CMCs. If the polymer shrinkage during curing results in a radial pressure p on the fibers, then τ_y should be replaced by μp because $\tau_i = \mu p$, where μ is the coefficient of sliding friction between the fiber and matrix (Kelly 1973). The equilibrium of forces, then, over a fiber length of $l/2$ gives

$$\sigma_f \frac{\pi d^2}{4} = \tau_y \pi d \frac{l}{2}$$

or

$$\frac{l}{d} = \frac{\sigma_f}{2\tau_y}.$$

We consider $l/2$ and not l because the fiber is being loaded from both ends. Given a sufficiently long fiber, it should be possible to load it to its breaking stress σ_{fu} by means of load transfer through the matrix flowing plastically around it. Let $(l/d)_c$ be the minimum fiber length-to-diameter ratio necessary to accomplish this. We call this ratio (l/d) the aspect ratio of a fiber and $(l/d)_c$ is the critical aspect ratio necessary to attain the breaking stress of the fiber, σ_{fu}. Then we can write

$$\left(\frac{l}{d}\right)_c = \frac{\sigma_{fu}}{2\tau_y}. \tag{10.76}$$

For a given fiber diameter d, we can think of a critical fiber length l_c. Thus,

$$\frac{l_c}{d} = \frac{\sigma_{fu}}{2\tau_y}. \tag{10.77}$$

Over a length l_c, the load in the fiber builds up from both ends. Strain builds in a likewise manner. Beyond l_c (i.e., in the middle portion of the fiber), the local displacements in the matrix and fiber are the same, and the fiber carries the major load while the matrix carries only a minor portion of the applied load. Equation (10.77) tells us that the fiber length l must be equal to or greater than l_c for the fiber to be loaded to its maximum stress, σ_{fu}. For $l < l_c$, the matrix will flow plastically around the fiber and will load it to a stress in its central portion given by

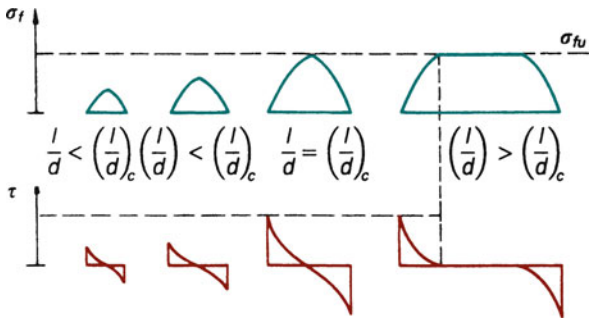

Fig. 10.17 Schematic of variation of tensile stress in a fiber (σ_f) and interface shear stress (τ) with different fiber aspect ratios (l/d)

$$\sigma_f = 2\tau\frac{l}{d} < \sigma_{fu} \tag{10.78}$$

This is shown in Fig. 10.17. An examination of this figure shows that even for $l/d > (l/d)_c$ the average stress in the fiber will be less than the maximum stress to which it is loaded in its central region. In fact, one can write for the average fiber stress

$$\overline{\sigma}_f = \frac{1}{l}\int_0^l \sigma_f \, dx = \frac{1}{l}\left[\sigma_f(l - l_c) + \beta\sigma_f l_c\right] = \frac{1}{l}\left[\sigma_f l - l_c\left(\sigma_f - \beta\sigma_f\right)\right]$$

or

$$\overline{\sigma}_f = \sigma_f\left(1 - \frac{1-\beta}{1/l_c}\right), \tag{10.79}$$

where $\beta\sigma_f$ is the average stress in the fiber over a portion $l_c/2$ of its length at both ends. One can thus regard β as a load transfer function. Its value will be precisely 0.5 for an ideally plastic material; that is, the increase in stress in the fiber over the portion $l_c/2$ will be linear. The longitudinal strength of a composite containing short but well aligned fibers will always be less than that of a composite containing unidirectionally aligned continuous fibers. For the strength of short fiber composite, per rule-of-mixtures, we can write:

$$\begin{aligned} \sigma_c &= \overline{\sigma}_f V_f + \sigma'_m V_m \\ \sigma_c &= \sigma_f V_f\left(1 - \frac{1-\beta}{1/l_c}\right) + \sigma'_m\left(1 - V_f\right). \end{aligned} \tag{10.80}$$

If $\beta = 0.5$,

$$\sigma_c = \sigma_f V_f \left(1 - \frac{l_c}{2l}\right) + \sigma'_m (1 - V_f),$$

where σ'_m is the in situ matrix stress at the strain under consideration. Suppose that in a whisker or short fiber reinforced metal the whiskers have an $l/l_c = 10$; then it can easily be shown that the strength of such a composite containing discontinuous but aligned fibers will be 95 % of that of a composite containing continuous fibers. Thus, as long as the fibers are reasonably long compared to the load transfer length, there is not much loss of strength owing to their discontinuous nature. The stress concentration effect at the ends of the discontinuous fibers has been neglected in this simple analysis.

10.5 Load Transfer in Particulate Composites

The shear lag model described in the previous section is suitable for explaining the load transfer from the matrix to a high aspect ratio reinforcement via shear along the interface parallel to the loading direction. No direct tensile loading of the reinforcement occurs. Such a model will not be expected to work for a particulate composite. A modified shear lag model (Fukuda and Chou 1981; Nardone and Prewo 1986) takes into account tensile loading at the particle ends. According to this modified shear lag model, the yield strength of a particulate composite is given by

$$\sigma_{\mathrm{yc}} = \sigma_{\mathrm{ym}}[1 + (L + t)/4L]V_{\mathrm{p}} + \sigma_{\mathrm{ym}}(1 - V_{\mathrm{p}}),$$

where σ_{ym} is the yield stress of the unreinforced matrix, V_{p} is the particle volume fraction, L is the length of the particle perpendicular to the applied load and t is the length of the particle parallel to the loading direction.

For the case of a composite with equiaxed particles (aspect ratio = 1), the above expression reduces to

$$\sigma_{\mathrm{yc}} = \sigma_{\mathrm{ym}}(1 + 0.5V_{\mathrm{p}}).$$

Note that this expression predicts a linear but modest increase in the strength of the composite with particle volume fraction. However, no account is taken of the particle size or other microstructural parameters.

Models involving the modified shear lag model, Eshelby's equivalent inclusion approach, and Weibull statistics have been proposed (Lewis and Withers 1995; Song et al. 2010). Incorporation of Weibull statistics (see Chap. 12) makes sense because the brittle, ceramic particles in a metallic matrix can debond and/or crack during deformation. The yield strength of the particulate MMC increases as the volume fraction and aspect ratio of the particles increase, while it decreases as the size of the SiC particles increases.

References

Arsenault RJ, Fisher RM (1983) Scripta Met 17:67
Behrens E (1968) J Composite Mater 2:2
Bhatt H, Donaldson KY, Hasselman DPH, Bhatt RT (1992) J Mater Sci 27:6653
Chamis CC (1983) NASA Tech. Memo. 83320, presented at the 38th annual conference of the Society of Plastics Industry (SPI), Houston, TX
Chamis CC, Sendecky GP (1968) J Compos Mater 2:332
Chawla KK (1973a) Metallography 6:155
Chawla KK (1973b) Philos Mag 28:401
Chawla KK (1974) In: Grain boundaries in engineering materials. Claitor's Publishing Division, Baton Rouge, LA, p 435
Chawla KK (1976a) J Mater Sci 11:1567
Chawla KK (1976b) In: Proceedings of the international conference on composite materials/1975, TMS-AIME, New York. p 535
Chawla KK, Metzger M (1972) J Mater Sci 7:34
Clingerman ML, King JA, Schulz KH, Meyers JD (2002) J Appl Polym Sci 83:1341
Cox HL (1952) Brit J Appl Phys 3:122
Day RJ, Robinson IM, Zakikhani M, Young RJ (1987) Polymer 28:1833
Day RJ, Piddock V, Taylor R, Young RJ, Zakikhani M (1989) J Mater Sci 24:2898
Dow NF (1963) General Electric Report No. R63-SD-61
Eshelby JD (1957) Proc R Soc A241:376
Eshelby JD (1959) Proc R Soc A252:561
Fukuda H, Chou TW (1981) J Compos Mater 15:79
Galiotis C, Robinson IM, Young RJ, Smith BJE, Batchelder DN (1985) Polym Commun 26:354
Gladysz GM, Chawla KK (2001) Composites A 32:173
Hale DK (1976) J Mater Sci 11:2105
Halpin JC, Kardos JL (1976) Polym Eng Sci 16:344
Halpin JC, Tsai SW (1967) Environmental factors estimation in composite materials design. AFML TR 67-423
Hashin Z, Rosen BW (1964) J Appl Mech 31:233
Hasselman DPH, Johnson LF (1987) J Compos Mater 27:508
Hill R (1964) J Mech Phys Solids 12:199
Hill R (1965) J Mech Phys Solids 13:189
Kardos JL (1971) CRC Crit Rev Solid State Sci 3:419
Kelly A (1970) Chemical and mechanical behavior of inorganic materials. Wiley-Interscience, New York, p 523
Kelly A (1973a) Strong solids, 2nd edn. Clarendon, Oxford, p 157
Kerner EH (1956) Proc Phys Soc Lond B69:808
Lewis CA, Withers PJ (1995) Acta Metall Mater 43:3685
Love AEH (1952) A treatise on the mathematical theory of elasticity, 4th edn. Dover, New York, p 144
Marom GD, Weinberg A (1975) J Mater Sci 10:1005
Mori T, Tanaka K (1973) Acta Metall 21:571
Nardone VC, Prewo KM (1986) Scripta Met 20:43
Nielsen LE (1974) Mechanical properties of polymers and composites, vol 2. Marcel Dekker, New York
Nye JF (1985) Physical properties of crystals. Oxford University Press, London, p 131
Poritsky H (1934) Physics 5:406
Reuss A (1929) Z Angew Math Mech 9:49
Rosen BW (1973) Composites 4:16
Rosen BW, Hashin Z (1970) Int J Eng Sci 8:157
Schadler LS, Galiotis C (1995) Int Mater Rev 40:116

Schapery RA (1969) J Compos Mater 2:311
Schuster DM, Scala E (1964) Trans Met Soc-AIME 230:1635
Song M, He Y, Fang S (2010) J Mater Sci 45:4097
Termonia Y (1987) J Mater Sci 22:504
Timoshenko S, Goodier JN (1951) Theory of elasticity. McGraw-Hill, New York, p 416
Turner PS (1946) J Res Natl Bur Stand 37:239
Vaidya RU, Chawla KK (1994) Compos Sci Technol 50:13
Vaidya RU, Venkatesh R, Chawla KK (1994) Composites 25:308
Vogelsang M, Arsenault RJ, Fisher RM (1986) Metall Trans A 7A:379
Voigt W (1910) Lehrbuch der Kristallphysik. Teubner, Leipzig
Weber L (2005) Acta Mater 53:1945
Weber L, Dorn J, Mortensen A (2003a) Acta Mater 51:3199
Weber L, Fischer C, Mortensen A (2003b) Acta Mater 51:495
J.M. Whitney (1973). J. Struct. Div., 113.
Xu ZR, Chawla KK, Mitra R, Fine ME (1994) Scripta Met Mater 31:1525
Yang X, Hu X, Day RJ, Young RJ (1992) J Mater Sci 27:1409
Young RJ, Day RJ, Zakikhani M (1990) J Mater Sci 25:127
Young RJ (1994) In: Chawla KK, Liaw PK, Fishman SG (eds) High-performance composites: commonalty of phenomena. TMS, Warrendale, PA. p 263

Further Reading

Herakovich CT (1998) Mechanics of fibrous composites. Wiley, New York
Kelly A (1973b) Strong solids, 2nd edn. Clarendon, Oxford
Nemat-Nasser S, Hori M (1993) Micromechanics: overall properties of heterogenous materials. North-Holland, Amsterdam
Tewary VK (1978) Mechanics of fibre composites. Halsted, New York

Problems

10.1. Describe some experimental methods of measuring void content in composites. Give the limitations of each method.

10.2. Consider a 40 % V_f SiC whisker-reinforced aluminum composite. $E_f = 400$ GPa, $E_m = 70$ GPa, and $(l/d) = 20$. Compute the longitudinal elastic modulus of this composite if all the whiskers are aligned in the longitudinal direction. Use Halpin-Tsai-Kardos equations. Take $\xi = 2(l/d)$.

10.3. A composite has 40 % V_f of a 150 μm diameter fiber. The fiber strength is 2 GPa, the matrix strength is 75 MPa, while the fiber/matrix interfacial strength is 50 MPa. Assuming a linear build up of stress from the two ends of a fiber, estimate the composite strength for (a) 200 mm long fibers and (b) 3 mm long fibers.

10.4. Derive the load transfer expression Eq. (10.62) using the boundary conditions. Show that average tensile stress in the fiber is given by Eq. (10.63).

10.5. Consider a fiber reinforced composite system in which the fiber has an aspect ratio of 1,000. Estimate the minimum interfacial shear strength τ_i, as a percentage of the tensile stress in fiber, σ_f, which is necessary to avoid interface failure in the composite.

10.6. Show that as $\xi \to 0$, the Halpin-Tsai equations reduce to

$$l/p = V_m/p_m + V_f/p_f$$

while as $\xi \to \infty$, they reduce to

$$p = V_m p_m + V_f p_f.$$

10.7. Consider an alumina fiber reinforced magnesium composite. Calculate the composite stress at the matrix yield strain. The matrix yield stress 180 MPa, $E_m = 70$ GPa, and $v = 0.3$. Take $V_f = 50$ %.

10.8. Estimate the aspect ratio and the critical aspect ratio for aligned SiC whiskers (5 μm diameter and 2 mm long) in an aluminum alloy matrix. Assume that the matrix alloy does not show much work hardening.

10.9. Alumina whiskers (density = 3.8 g/cm^3) are incorporated in a resin matrix (density = 1.3 g/cm^3). What is the density of the composite? Take $V_f = 0.35$. What is the relative mass of the whiskers?

10.10. Consider a composite made of aligned, continuous boron fibers in an aluminum matrix. Compute the elastic moduli, parallel, and transverse to the fibers. Take $V_f = 0.50$.

10.11. Fractographic observations on a fiber composite showed that the average fiber pullout length was 0.5 mm. If $V_{fu} = 1$ GPa and the fiber diameter is 100 μm, calculate the strength of the interface in shear.

10.12. Consider a tungsten/copper composite with following characteristics: fiber fracture strength = 3 GPa, fiber diameter = 200 μm, and the matrix shear yield strength = 80 MPa. Estimate the critical fiber length which will make it possible that the maximum load bearing capacity of the fiber is utilized.

10.13. Carbon fibers ($V_f = 50$ %) and polyimide matrix have the following parameters:

$$E_f = 280\,\text{GPa} \quad E_m = 276\,\text{MPa}$$
$$v_f = 0.2 \quad v_m = 0.3$$

(a) Compute the elastic modulus in the fiber direction, E_{11}, and transverse to the fiber direction, E_{22}.

(b) Compute the Poisson ratios, v_{12} and v_{21}.

10.14. Copper or aluminum wires with steel cores are used for electrical power transmission. Consider a Cu/steel composite wire having the following data:

inner diameter = 1 mm
outer diameter = 2 mm

$$E_{Cu} = 150 \text{ GPa} \qquad \alpha_{Cu} = 16 \times 10^{-6}\,K^{-1}$$
$$E_{steel} = 210 \text{ GPa} \qquad \alpha_{steel} = 11 \times 10^{-6}\,K^{-1}$$
$$\sigma_{yCu} = 100 \text{ MPa} \qquad v_{Cu} = v_{steel} = 0.3$$
$$\sigma_{ysteel} = 200 \text{ MPa}$$

(a) The composite wire is loaded in tension. Which of the two components will yield plastically first? Why?
(b) Compute the tensile load that the wire will support before any plastic strain occurs.
(c) Compute the Young's modulus and CTE of the composite wire.

10.15. A composite is made of unidirectionally aligned carbon fibers in a glass-ceramic matrix. The following data are available:

$$E_{f1} = 280 \text{ GPa}, E_{f2} = 40 \text{ GPa}, \; E_m = 70 \text{ GPa}$$
$$v_{f1} = 0.2 \quad v_m = 0.3$$
$$G_{f12} = 18 \text{ GPa}$$

(a) Compute the elastic modulus in the longitudinal and transverse directions.
(b) Compute the two Poisson's ratios.
(c) Compute the principal shear modulus, G_{12}.